REMARKS

Reconsideration and withdrawal of the rejections set forth in the Office action dated May 9, 2006 are respectfully requested. Applicants petition the Commissioner for a 1-month extension of time. A separate petition accompanies this amendment.

I. Amendments

Claims 1, 10, and 40 are amended in accord with the Examiner's kind suggestions.

Claims 1, 26 are amended to recite a step of detecting binding of the test agent based on the membrane fluidity evaluated.

Claims 4 and 29 are amended to recite a label associated with the lipid bilayer expanse(s).

Claims 36 and 39 are amended to change the reference to "a cell vesicle" to a "plasma membrane vesicle" as known in the art.

New claims 42 and 43 find basis in paragraphs [0012] and [0045] of the published application.

No new matter is added by way of these amendments.

II. Objection to the Claims

Claim 1 was objected to as allegedly unclear whether lines 7-8 are intended to be a method step or are reciting further components of the surface detector array device of line 3. Claim 1 is further objected to for consistency in claim terminology. Claim 1 is amended in accord with the Examiner's kind suggestions.

Claim 10 was objected to for grammatical reasons. The claim is amended in accord with the Examiner's kind suggestion.

Claim 40 was objected to for grammatical reasons. Applicants have amended the claim in accord with the Examiner's kind suggestion.

In view of the above, Applicants respectfully request withdrawal of the objections to the claims.

III. Rejections under 35 U.S.C. §112, first paragraph

Claims 4-7 were rejected under 35 U.S.C. § 112, first paragraph, for failing to comply with the written description requirement.

Claims 1-7, 10, 34-36, and 40 were rejected under 35 U.S.C. § 112, first paragraph, for lack of written description.

Claims 1-7, 10, 34-36, and 40 were further rejected under 35 U.S.C. §112, first paragraph, allegedly because the specification does not enable any person skilled in the art to which it pertains, or with which it is most connected to make and use the invention commensurate in scope with the claims.

A. Written Description

1. Claims 4-7

Claim 4 is amended to clarify that the label is associated with the lipid bilayer expanses. As recited in claims 5 and 6, the label may be attached to the lipid bilayer component or it may be attached to a background membrane component.

2. Claims 1-7, 10, 34-36, and 40

The Examiner asserts that the specification fails to provide an adequate written description of the invention as claimed. The claims, as amended, are directed to a method for assaying an interaction between a test agent and a lipid-bilayer-associated component. The method comprises providing a surface detector array device having one or more bilayer-compatible surface regions including a component associated with the lipid bilayer expanse. The device is contacted with a bulk aqueous phase comprising the test agent which binds to the lipid bilayer-associated component. The membrane fluidity of one or more of the lipid expanses is decreased by this binding. The membrane fluidity is evaluated and binding of the test agent and the lipid bilayer-associated component is determined.

Without being limited to theory, Applicants believe that the decrease in membrane fluidity results from cooperative binding between the test agent and the

lipid bilayer-associated component, that is, ligand binding causes an aggregation of the membrane component. This cooperative binding should work with any test agent, including cholera toxin, the surface of a cell, liposomes or any of the other test agents claimed. Indeed, even monomeric growth factor proteins cause aggregation of receptor tyrosine kinases (RTKs). So, even if the ligand is not polyvalent, as long as it induces cooperative binding (aggregation) of the lipid bilayer-associated component, then there should be a decrease in membrane fluidity upon binding. Additionally, small molecules induce aggregation/oligomerization of the membrane component as evidenced by the following references (copies enclosed) which present evidence that small molecules can induce oligomerization/aggregation of G protein-coupled receptors:

> 1) Angers et al. (2000) Proc. Natl. Acad. Sci. USA 97, 3684-3689;
>
> 2) Wurch et al. (2001) FEBS Lett. 507, 109-113; and
>
> 3) Gines et al. (2000) Proc. Natl. Acad. Sci. USA 97, 8606-8611.

As shown in these references, certain small molecules can induce the aggregation of their respective receptors. Therefore, small molecules would be expected by one skilled in the art to decrease membrane fluidity. Accordingly, one skilled in the art would recognize that binding of small molecules would affect the membrane fluidity of the bilayer.

a. Legal Standard for Written Description

According to M.P.E.P. § 2163.02, an objective standard for determining compliance with the written description requirement is, "does the description clearly allow persons of skill in the art to recognize that he or she invented what is claimed." *In re Gosteli*, 872 F.2d 1008, 1012, 10 USPQ2d 1614, 1618 (Fed. Cir. 1991). An applicant shows possession of the claimed invention by describing the claimed invention with all of its limitations using such descriptive means as words, structures, figures, diagrams and formulas that fully set forth the claimed invention.

Lockwood v. American Airlines, Inc., 107 F.3d 1565, 1572, 41 USPQ2d 1961, 1966 (Fed. Cir. 1997).

Unlike the "enablement" requirement, the "written description" requirement of 35 U.S.C. §112, first paragraph is not concerned with support commensurate with the breadth of the claims. The essential purpose of the written description requirement is to show the possession of the invention as of the filing date as a *prima facie* date of invention. *In re Smith*, 481 F.2d 910, 178 U.S.P.Q. 620, 623 (CCPA 1973). Accordingly, the specification is required to contain a statement that adequately describes the invention as claimed. However, the invention need not be described in *ipsis verbis* in order to satisfy the description requirement. See *In re Lukach, Olson, and Spurlin*, 169 U.S.P.Q. 795, 796 (CCPA 1971).

"It is not required that the application describe the claim limitations in greater detail than the invention warrants. The description must be sufficiently clear that persons of skill in the art will recognize that the applicant made the invention having those limitations." *Martin v. Mayer*, 823 F.2d 500, 3 USPQ2d 1333 (Fed. Cir. 1987).

b. Meeting the Legal Standard

First, the Examiner states "there is no recited correlation between evaluation and detection in the claim." Applicants' amended claims specifically recite a detection step, where binding of the test agent and the lipid bilayer-associated components is correlated to membrane fluidity.

Next, the Examiner states that the claims are drawn to "a genus of test agents and lipid bilayer-associate components" (Office action dated May 9, 2006, page 7). As noted above, Applicants believe that the decrease in membrane fluidity as shown in the examples with cholera toxin results from cooperative binding between the test agent and the lipid bilayer-associated component, that is, ligand binding causes an aggregation of the membrane component. One skilled in the art would readily recognize that this cooperative binding should work with any test agent, including cholera toxin, the surface of a cell, liposomes or any of the

other test agents claimed. As also shown above, and evidenced by the enclosed articles, small molecules induce aggregation/oligomerization of the membrane component. In view of the similar mechanism of action, Applicants have enabled one skilled in the art to make and use the present method with the entire genus as presently claimed.

Finally, claim 3 is amended to correctly recite that the bacterial endotoxin is the lipid bilayer-associated component. The Examiner is respectfully directed to paragraph [0163] of the published application where endotoxins are described as a membrane component (the lipid bilayer-associated component) that binds to the test agent.

In view of the teachings in the specification, the level of skill, and the knowledge in the art, one skilled in the art would reasonably conclude that Applicants were in possession of the claimed invention at the time the invention was filed.

B. Enablement

The first paragraph of 35 U.S.C. §112 requires that the specification of a patent enable any person skilled in the art to which it pertains to make and use the claimed invention without undue experimentation (e.g., *In re Vaeck*, 947 F.2d 488, 20 USPQ2d 1438 (Fed. Cir. 1991).

The enablement requirement is met if the description enables any mode of making and using the claimed invention (*Engel Industries, Inc. v. Lockformer Co.*, 946 F.2d 1528, 20 USPQ2d 1300 (Fed. Cir. 1991).

An invention is enabled even though the disclosure may require some routine experimentation to practice the invention. *Hybritech Inc, V. Monoclonal Antibodies, Inc.*, 802 F.2d 1367, 1384, 231 U.S.P.Q. 81, 94 (Fed. Cir. 1986). The fact that the required experimentation may be complex does not necessarily make it undue, if the art typically engages in such experimentation. *MLT. v A.B. Fortia*, 774 F.2d 1104, 227 U.S.P.Q. 428 (Fed. Cir. 1985).

As noted above, the amended claims are directed to a method for assaying an interaction between a test agent and a lipid bilayer-associated component using a surface detector array device including a plurality of lipid bilayer expanses. When the test agent binds to the lipid bilayer-associated component, the membrane fluidity of the lipid bilayer expanse(s) is decreased. Example 7 of the present invention provides guidance for an _exemplary_ polyvalent test agent and lipid bilayer-associated component, specifically the cholera toxin and the ganglioside GM1 membrane target. As noted above, Applicants believe that cooperative binding between the test agent and the lipid bilayer-associated component, that is, ligand binding causes an aggregation of the membrane component

Accordingly, Applicants submit that the specification would enable any person skilled in the art to which it pertains to make and use the claimed invention.

In light of the above, Applicants submit that the present claims satisfy the requirements of 35 U.S.C. §112, first paragraph and respectfully request that the rejections be withdrawn.

IV. Rejection under 35 U.S.C. §112, second paragraph

Claims 1-7, 10, 34-36, and 40 were rejected under 35 U.S.C. §112, second paragraph as allegedly indefinite for failing to particularly point out and distinctly claim the subject matter which the applicant regards as the invention. The Examiner had four specific objections, which are set forth and discussed below.

1. The Examiner objected to claim 1 as allegedly incomplete for omitting essential steps. Claim 1 recites a step of evaluating the membrane fluidity of one or more of the lipid bilayer expanses. Claim 1 is amended to recite a step of correlating the detected membrane fluidity with binding of the test agent and the lipid bilayer-associated component. Thus, claim 1 recites all the necessary steps involved in the method.

2. The Examiner objected to claims 4-7 as allegedly indefinite. Specifically, claim 4 recites that the lipid bilayer-associated component is a label. As noted

above, claim 4 is amended to properly recite that the label is associated with one or more of the lipid bilayer expanses.

3. Claim 36 was objected to for the language "cell-vesicle" as allegedly unclear. Applicants have amended the claim to remove reference to a cell-vesicle and have instead made reference to a plasma membrane vesicle. This term is known in the art as evidenced by a search in the PubMed publications database (http://www.ncbi.nlm.nih.gov/entrez/) for "plasma membrane vesicle," which yielded 46 articles that reference the term.

4. Claim 36 was additionally objected to for the language "giant" as a relative term that allegedly renders the claim indefinite. Applicants respectfully submit that the term "giant liposome" is standard in the art and is understood to refer to liposomes with a diameter greater than large unilamellar liposomes or about 10 µm or greater. Applicants refer the Examiner to a review article (Segota, et al., Advances in Colloid and Interface Science, 2006) describing the use of giant liposomes (article enclosed) in the section 2.2 on Nomenclature.

In light of the above amendments, the teaching in the specification, and/or the knowledge of those skilled in the art, Applicants respectfully request withdrawal of the rejections under 35 U.S.C. §112, second paragraph.

V. Rejections under 35 U.S.C. §103

Claims 1-2, 4-6, 10, and 34-36 were rejected under 35 U.S.C. §103 as allegedly obvious over Boxer et al. (the '326 patent), or, alternatively, Boxer et al. (the '948 publication) in view of Groves et al. (Science, 275:651-653, 1997).

Claim 3 was rejected under 35 U.S.C. §103 as allegedly obvious over Boxer et al. (the '326 patent), or, alternatively, Boxer et al. (PCT Publication No. WO 98/23948) in view of Groves et al., and further in view of Gutsmann et al. (Biophysical Journal, 80:2935-2945, 2001).

Claim 7 was rejected under 35 U.S.C. §103 as allegedly obvious over Boxer et al. (the '326 patent), or, alternatively, Boxer et al. (PCT Publication No. WO 98/23948)

in view of Groves *et al.* and further in view of Salafsky *et al.* (Biochemistry, 35:14773-14781, 1996).

Claim 40 was rejected under 35 U.S.C. §103 as allegedly obvious over Boxer *et al.* (the '326 patent), or, alternatively, Boxer *et al.* (PCT Publication No. WO 98/23948) in view of Groves *et al.*, and further in view of Keinanen *et al.* (U.S. Patent No. 6,235,535).

These rejections are respectfully traversed.

A. <u>The Present Claims</u>

The present method as embodied by claim 1 comprises a method for assaying an interaction between a test agent and a lipid bilayer-associated component. The method comprises (i) providing a surface detector array device comprising (a) a substrate having a surface defining a plurality of distinct bilayer-compatible surface regions separated by one or more bilayer barrier regions, (b) a plurality of lipid bilayer expanses localized above the plurality of distinct bilayer-compatible surface regions, the lipid bilayer expanses having a component associated with the lipid bilayer expanse; (iii) contacting the device with a bulk aqueous phase comprising a test agent that specifically binds to the lipid bilayer-associated component, whereby the membrane fluidity of at least one of the plurality of lipid bilayer expanses decreases when said test agent binds to said lipid bilayer-associated component; (iv) evaluating the membrane fluidity of one or more of the lipid bilayer expanses, and detecting binding of the test agent to the lipid bilayer-associated component by correlating a decrease in membrane fluidity to binding.

B. <u>The Cited References</u>

<u>BOXER ET AL., THE '326 PATENT</u> relate to a surface detector array device, comprising (i) a substrate having a surface defining a plurality of distinct bilayer-compatible surface regions separated by one or more bilayer barrier regions, (ii) a lipid bilayer expanse stably localized on each of said bilayer-compatible surface

regions, (iii) an aqueous film interposed between each bilayer-compatible surface region and corresponding lipid bilayer expanse, wherein each lipid bilayer expanse is stably localized above each bilayer-compatible surface, and (iv) a bulk aqueous phase covering the lipid bilayer expanses.

BOXER ET AL., THE '948 PUBLICATION corresponds to the '326 patent for purposes of the Examiner's rejections and is thus, not separately discussed.

GROVES ET AL. describe partition supported lipid bilayers on arrays. The lipid bilayers are confined by the barriers. The bilayers retain lateral fluidity within the "corrals."

GUTSMANN ET AL. investigate the relationship between the interaction of CAP-18-derived peptides with membranes and the activity of the peptides.

SALAFSKY ET AL. describe a method for creating fluid supported bilayers which contain oriented and functional photosynthetic reaction centers.

KEINANEN ET AL. relate to a fluorescence-based immunoassay method for the detection of an analyte. The method includes attaching receptor molecules to a lipid membrane, contacting a sample with the receptor molecules, and measuring the fluorescence change caused by a change of aggregation level of the receptor molecules.

C. Analysis

According to the M.P.E.P. § 2143, "to establish a prima facie case of obviousness, three basic criteria must be met. First, there must be some suggestion or motivation, either in the references themselves or in the knowledge generally available to one of ordinary skill in the art, to modify the reference or to combine reference teachings. Second, there must be a reasonable expectation of success. Third, the prior art references (or references when combined) must teach or suggest all the claim limitations."

1. Rejection of claims 1-2, 4-6, 10, and 34-36

The combination of Boxer *et al.* and Groves *et al.* fail to teach a method for assaying an interaction between a test agent and a lipid bilayer-associated component including evaluating the membrane fluidity of one or more of the lipid bilayer expanses and detecting binding of the test agent to the lipid bilayer-associated component by correlating a decrease in membrane fluidity to binding.

2. Rejection of claim 3

The deficiencies of the '326 patent and Groves *et al.* are described above. Nor does Gutsmann *et al.* provide the missing teaching. Instead, Gutsmann *et al.* describe several biophysical techniques to investigate the interaction of CAP-18 peptides and a membrane but make no mention of evaluating the fluidity of the membrane.

3. Rejection of claim 7

The deficiencies of the '326 patent and Groves *et al.* are described above. Salafsky *et al.* is cited merely for a teaching of attachment of labels and makes no mention of evaluating membrane fluidity and detecting binding by correlating a decrease in membrane fluidity to binding.

4. Rejection of claim 40

The deficiencies of the '326 patent and Groves *et al.* are described above.

Nor does Keinanen *et al.* supply the missing teaching. Instead, Keinanen *et al.* teach detecting analyte-receptor binding by fluorescence changes by aggregation of the receptors when bound to a multivalent analyte and make no mention of evaluating membrane fluidity or detecting binding based on the membrane fluidity.

As the references, alone or in combination, fail to teach or suggest all the claim limitations, Applicants respectfully request withdrawal of the rejections under 35 U.S.C. § 103.

VI. Obviousness-Type Double Patenting Rejections

Claims 1-2, 4-7, 10, 34-36 and 40 were rejected under the judicially created doctrine of obviousness-type double patenting as being directed to an invention not patentably distinct from claims 22-26 of co-owned patent no. 6,699,719 in view of Groves *et al.*

A. The Present Claims

The present application comprises a method for assaying an interaction between a test agent and a lipid bilayer-associated component. The method comprises (i) providing a surface detector array device comprising (a) a substrate having a surface defining a plurality of distinct bilayer-compatible surface regions separated by one or more bilayer barrier regions, (b) a plurality of lipid bilayer expanses localized above the plurality of distinct bilayer-compatible surface regions, the lipid bilayer expanses having a component associated with the lipid bilayer expanse; (iii) contacting the device with a bulk aqueous phase comprising a test agent that specifically binds to the lipid bilayer-associated component, whereby the membrane fluidity of at least one of the plurality of lipid bilayer expanses decreases when said test agent binds to said lipid bilayer-associated component; (iv) evaluating the membrane fluidity of one or more of the lipid bilayer expanses, and detecting binding of the test agent to the lipid bilayer-associated component by correlating a decrease in membrane fluidity to binding.

B. U.S. Patent No. 6,699,719 (the '719 patent)

The '719 patent relates to a multiplexed assay, comprising the steps of:

(i) providing a surface detection array device, said device comprising a substrate having a surface defining a plurality of distinct bilayer-compatible surface regions separated by one or more bilayer barrier regions, said bilayer-compatible surface regions and said bilayer barrier regions being formed of different materials, a first lipid bilayer expanse having a first composition and stably localized above a first of said plurality of distinct bilayer-compatible surface regions, a second lipid

bilayer expanse having a second composition different from said first composition and stably localized above a second of said plurality of distinct bilayer-compatible surface regions, wherein each of said expanses is localized above each of said surface regions in the absence of covalent linkages between each of said lipid bilayer expanses and each of said bilayer-compatible surface regions, and is separated therefrom by an aqueous film interposed between said bilayer-compatible surface regions and said corresponding lipid bilayer expanses;

(ii) contacting said device with a bulk aqueous phase comprising a test agent; and

(iii) assaying an interaction between said test agent and said first composition and an interaction between said test agent and said second composition.

C. Analysis

The purpose of obviousness-type double patenting is to prevent improper timewise extension of patent rights by prohibiting the issuance of claims in a second application which are not "patentably distinct" from the claims of the first patent. M.P.E.P. 804(II)(B)

The present method requires a step of evaluating the membrane fluidity of one or more of the lipid bilayer expanses and detecting binding of the test agent to the lipid bilayer-associated component by correlating a decrease in membrane fluidity to binding. Thus, the present method evaluates a membrane property, namely membrane fluidity, in order to assay the interaction of the test agent and the lipid bilayer-associated component. This feature is not an obvious variation of the "assaying an interaction between said test agent and said first composition and an interaction between said test agent and said second composition."

Accordingly, Applicants respectfully request withdrawal of the obviousness-type double patenting rejections.

VII. Conclusion

Applicants respectfully submit that the pending claims are in condition for immediate allowance. The undersigned invites the Examiner to call (650) 838-4410 with any questions or comments. The Commissioner is hereby authorized and requested to charge any deficiency in fees herein to Deposit Account No. 50-2207.

Respectfully submitted,
Perkins Coie LLP

Date:____Sept. 11, 2006____

Jacqueline F. Mahoney
Registration No. 48,390

Correspondence Address:
Customer No. 22918

ELSEVIER

Review

Spontaneous formation of vesicles

Suzana Šegota, Đurđica Težak *

Department of Chemistry, University of Zagreb, Faculty of Science, Horvatovac 102a, P.O. Box 163, 10001 Zagreb, Croatia

Abstract

This review highlights the relevant issues of spontaneous formation of vesicles. Both the common characteristics and the differences between liposomes and vesicles are given. The basic concept of the molecular packing parameter as a precondition of vesicles formation is discussed in terms of geometrical factors, including the volume and critical length of the amphiphile hydrocarbon chain. According to theoretical considerations, the formation of vesicles occurs in the systems with packing parameters between 1/2 and 1.

Using common as well as new methods of vesicle preparation, a variety of structures is described, and their nomenclature is given. With respect to sizes, shapes and inner structures, vesicles structures can be formed as a result of self-organisation of curved bilayers into unilamellar and multilamellar closed soft particles. Small, large and giant uni-, oligo-, or multilamellar vesicles can be distinguished. Techniques for determination of the structure and properties of vesicles are described as visual observations by optical and electron microscopy as well as the scattering techniques, notably dynamic light scattering, small angle X-ray and neutron scattering. Some theoretical aspects are described in short, viz., the scattering and the inverse scattering problem, angular and time dependence of the scattering intensity, the principles of indirect Fourier transformation, and the determination of electron density of the system by deconvolution of $p(r)$ function. Spontaneous formation of vesicles was mainly investigated in catanionic mixtures. A number of references are given in the review.
© 2006 Elsevier B.V. All rights reserved.

Keywords: Catanionic mixtures; Liposomes; Mixed systems; Packing parameters; Scattering techniques; Spontaneous vesicle formation; Vesicles

Contents

* Corresponding author. Tel.: +385 1 4606141; fax: +385 1 4606131.
  E-mail address: djurdjicatezak@yahoo.com (Đ. Težak).

1. Introduction

1.1. Historical aspects of liposomes and vesicles

Because of their chemical structure, surface-active substances, amphiphiles, show the ability of self-organisation in the solvents, forming self-assemblies with a large variety of morphologically different structures [1]. The phase behaviour of surfactant systems and their corresponding static structures have been most studied. However, the morphological dynamics of these processes is not only of fundamental interest, but it plays an important role in many technological applications. Several products rely on their colloidal, chemical, microencapsulating and surface properties; these products range from drug-dosage forms (antifungals, anticancer agents, vaccines) and cosmetic formulations (skin-care products, shampoos) to diagnostics and various uses in the food industry, etc. [2–10]. Knowledge about the dynamics of formation, and the structure of aggregates, makes it possible to control further processes [11]. Properties of the system depend strongly on sample preparation. Morphological transitions in surfactant systems can be triggered by a large variety of parameters, e.g., by mixing processes, dilution, changes in the solution composition, or chemical reaction, and by changes in either temperature or pressure [12,13]. However, morphological transitions may also be induced by applying external fields such as shear, electric or magnetic fields. In order to gain a full understanding of either the morphology of the initial structure or the appearance of a newly formed one, appropriate experimental techniques provide sufficiently detailed structural information. Common methods are typically either direct visualisation (optical or electron microscopy) or scattering techniques (light scattering, LS, small angle neutron scattering, SANS, small angle X-ray scattering, SAXS).

In this review, the methods of vesicles preparation, spontaneous formation of catanionic vesicles, and the methods for structural observations will be described.

Some facts about liposomes and vesicles have to be emphasised; the difference is due to the chemical composition of amphiphilic molecules. Liposomes are formed from phospholipid molecules and are called lipid vesicles, sometimes simply vesicles; they are supramolecular assemblies of amphiphiles that contain two hydrophilic tails and one hydrophobic head group. Other vesicles, lamellar bilayers and multilayers are formed from different surfactants.

The discovery of liposomes is attributed to A.D. Bangham, who performed research on blood and blood clots in 1961, particularly on the colloid behaviour of lecithin and other phospholipids. He found that phospholipids form spheres in the diluted aqueous solutions [14]. Citing Bangham's paper, these spheres were described as, "Liposomes are the smallest artificial vesicles of spherical shape that can be produced from natural nontoxic phospholipids and cholesterol. Liposomes are microscopic, fluid-filled pouches whose walls are made of layers of phospholipids identical to the phospholipids that make up cell membranes." The appearance and permeability of the phospholipids membranes were similar to the properties of biological membranes. For that reason, liposome research was used as the model for biological membranes. Liposomes are characterised by their size, the number of layers, and by their surface charge. According to the surface charge sign, they are classified as anionic, cationic and neutral liposomes. Although the discovery of lipid vesicles in the early 1960s was made by Bangham, papers about the colloid behaviour of lecithin and other phospholipids can be found much earlier. In 1811, Vauquelin described the bonding of phosphorus onto the fatty acids within the material isolated from the brain using hot ethanol [15]. Cylindrical structures that were growing very fast from thin layers exhibiting nice colours under crossed polarisers were investigated. In that research, lipids extracted from brain tissue were mostly used. Firstly, their structures and shapes were observed from dried myelin material that Lehman named myelin figures [15]. Gobley described the presence of a lipid substance in the chick brain containing phosphorus similar to that present in the egg yolk [16]. Lehmann investigated patterns by polarisation microscopy; today, these patterns are called big multilamellar vesicles [17]. Mechanical stress as well as crystal defects caused some of the cylinders to grow, and being detached from the original lipid material, they closed the outer angles forming suspended colloid particles—liposomes.

Introduction of the electron microscope, more than a hundred years later, made it possible to understand that those particles are closed structures containing in their inner part a liquid that can diffuse freely. Former experiments claimed that

swelling of lipids in contact with water is a consequence of the fast penetration of water into their crystal lattice [18]. Amphiphilic properties and the structure of the lipid double layer, as well as the properties of biomembranes, were recognised in the 1920s by studying the colloid behaviour of lipid dispersions [19]. But the biological importance of aqueous lipid systems was not recognised because the results were not reproducible. Today, it is known that the low reproducibility was caused by impurities within the lipids. Minor contamination with charged lipids can drastically change their swelling and other colloidal properties. Therefore, many colloid chemists worked mostly with much more reliable metal oxide or silver halide colloids [20–22]. Besides, experiments with large multilamellar vesicles or lecithin (or some other phospholipids) gave no useful information; for this reason, that research could not be applied to blood clotting. But such research enabled the characterisation of liposomes as self-enclosed artificial membranes [15]. Using osmotic and permeability experiments, Bangham showed that the lecithin particles catch water fractions, while the phospholipid bilayers play the role of semipermeable membranes [23]. This finding changed the conception of liposomes, since until that time they were considered as a kind of colloid dispersions. In the 1950s, scientists reported on vesicles formation by sonication of the lecithin sol, and on their "molecular mass", but they named these particles "micelles" [24–26]. They used these suspensions in many experiments, e.g., reduction of blood cholesterol by sonicated oral lipid dispersions [27]. Bangham determined the physico-chemical properties of particles, including particle size distribution, osmotic behaviour, and surface charge of the colloidal mesophases [15]. Due to the high heterogeneity of size distribution, those dispersions did not find application in experiments with blood proteins. Small vesicles prepared by sonication of large liposomes found a much wider application; the achieved reproducibility was much better [28–33].

During the 1970s, the packing potential, i.e., the importance of encapsulation in drug delivery was recognised [34,35]. Due to the ability of embedding the drug into the inner part of liposomes, many drugs were better prepared. In the 1980s, investigations were focused on applications requiring injection of liposomes into the blood circulation, and liposomes delivery directly to the specific location [36–45]. When delivered systemically, liposomes are subjects to distribution by the circulatory system, and they are rapidly eliminated by the liver. The following decade was characterised by the use of the liposome technology in gene diagnosis and gene therapy [2–9].

Today, liposomes are very useful models, reagents and tools in various scientific fields, including mathematics and theoretical physics (topology of two-dimensional surfaces floating in a three-dimensional continuum), biophysics (properties of cell membranes and channels), biology (biomembrane and inner parts of cells, excretion, cell function, trafficking and signalling, gene delivery and function), biochemistry (functions of membrane proteins), chemistry (catalysis, energy conversion, photosynthesis), and colloid chemistry (stability, thermody-

namics) [2–9,46]. Publications of Kaler et al. introduced the research on the vesicles formation [47–49]. Their investigations on the systems of aqueous dispersions of liquid crystals of the double-tailed surfactant sodium 4-(1'-heptylnonyl)benzenesulfonate (SHBS) include the characterization and aging of vesicular dispersions, determination of vesicular sizes as well as the investigations of the ionic permeability of vesicles [47–49]. They found the spontaneously formed vesicles in aqueous mixtures of single-tailed surfactants [50], but these vesicles tend not to be able to encapsulate an aqueous interior phase. The stability is enhanced via polymerization of monomers, such as sryrene, trapped in the membrane [51]. Kaler's work and the important contribution on the field of the spontaneous formation of vesicles is through the review discussed.

Some surfactant structures can mimic the biological ones. Therefore, surfactants in aqueous solutions constitute important model systems for the research on enzymes and biomembranes. A new field was developed in chemistry, the so-called mimetic chemistry [52], which deals with the models mimicking biomembranes by researching their structures as well as the mechanisms and function both in vivo and in vitro.

It should be pointed out that the field of vesicles and liposomes investigation is huge and developing, and the present review can be neither comprehensive nor final.

1.2. Molecules forming vesicles

Vesicular dispersions have been studied intensively as model systems in research on permeable biological membranes in which different drugs were embedded [53], as well as on the formation of cells, and fluctuations of their shapes [54]. Pharmaceutical and cosmetic industries are very interested in vesicle research [55–57]. Since the drug can be captured into the vesicle, the control of the drug action is possible at a particular place in the body. In addition, production of ultra-fine vesicles is extremely useful for the membrane micro-reactors [58,59].

With regard to the molecular structure, several main classes of molecules forming vesicles can be distinguished [60]:

- Vesicles formed from aqueous dispersions of phospholipids or their mixtures, named liposomes or lipid vesicles [56,61–65]. They can be metastable structures of a high kinetic stability [11,66] (but not thermodynamic stability), because their formation usually requires some energy input. They can be formed by common preparation methods, e.g., sonication, electroformation, or extrusion from diluted lamellar dispersions [28–33,67–69];
- Vesicles formed from glycolipids that are mainly natural extracts [70], and from synthetic glycolipids [71–73]. Glycolipids are one of the major components of cell membranes; understanding and control of interglycolipid vesicle interaction [74] present the key for achieving the application of glycolipids in drug delivery systems [75] and other aspects of biotechnology [76]. Baba et al. have investigated recently the effect of pH and NaCl concentration on the colloidal stability of $Mal_3(Phyt)_2$ vesicles [77].

Recently, the effect of glycolipid structure, concentration, and the pore size of the extrusion membrane on vesicle size and their stability were investigated by dynamic light scattering [78]. It was shown that the glycolipid structure and concentration play an important role in the vesicle stability. Maurer et al. have shown that surfactant lipid IV_A, a bioactive precursor of lipid A, forms unilamellar vesicles [79]. Glycolipids belong to one of four categories of biosurfactants which are divided on the basis on the structure of their hydrophilic part. Fatty acids, lipopeptides and polymers belong to the other categories. Functions and potential applications of glycolipid biosurfactants, the key features of their biosynthesis, and their physicochemical and bioactive properties have been summarised in two reviews recently published [80 81].

- Vesicles formed from double-chain dialkyldimethylammonium surfactants with hydroxide, acetate, or halide, usually bromide or chloride counterions [82–93];
- Vesicles formed within aqueous mixtures of oppositely charged surfactants, the so-called catanionic vesicles [94–101]. Besides, this group includes mixtures of cationic surfactants and anionic poly-electrolytes [102–105]. Recently, spontaneous formation of vesicles in the catanionic mixture of SDBS/DDAB/H_2O was detected using transmission electron microscopy at cryogenic temperatures, Cryo-TEM, light microscopy, SAXS and dynamic light scattering, DLS [106]. Both unilamellar and multilamellar vesicles were found, with coacervates as the precursor phase. Stable self-assembled structures and the properties in excess of and salt-free catanionic surfactant solution were reviewed and summarized recently [12,107].
- Vesicles formed in multicomponent systems including nonionic surfactant/cosurfactant/water (sometimes seawater), and sometimes with a small quantity of an ionic cosurfactant added [108–114], constitute the group of surfactant vesicles with incorporated polymers aimed at increasing their thermodynamic stability, and achieving a monodisperse population of vesicles [115–118].

In the last few years, spontaneous vesicle formation from a mixture of a zwitterionic surfactant and an anionic surfactant [119,120], from homopolymer polyelectrolytes [121], from lipids [122–125], and from the novel gemini surfactant systems [126–128] has been reported. Recently, bolamphiphiles have been introduced as a new class of amphiphiles forming vesicles of increased thermostability compared to cationic vesicles [97,129–132].

2. The concept of molecular packing parameter

Self-organising of amphiphiles in solution is spontaneous and thermodynamically driven, and it depends on their molecular structure. These phenomena were described by the concept of molecular packing parameter, introduced by Israelachvili et al. [133–138]. This concept, based on geometrical considerations, makes it possible to assume the shape and size of equilibrium associates. Shapes of the spontaneously formed association colloids can be predicted with considerable certainty using three nominal geometric parameters of the surfactant molecule:

- polar head surface, a
- tail volume, v
- chain length, l.

Surfactant molecular clusters of association colloids can be formed as micelles, inverted micelles, liquid crystals, bilayers–lamellae, vesicles, liposomes, and microemulsions [135,139,140]. At air/water interfaces, surfactants form monolayers due to specific adsorption on the interface. Colloid structures formed in the aqueous solutions of surfactants reveal physical interactions between the molecules, but no chemical interactions.

Due to the hydrophilic/hydrophobic properties of amphiphilic molecules, self-organisation in the solutions can be observed through various morphological structures. The driving force in the association of amphiphilic molecules, as well as in the aggregation of primary associates (micelles, vesicles), is the tendency of the hydrophobic part to minimise the contact with water; this is the so-called hydrophobic effect. Shapes of the observed associates, spheres, rods, and bilayers, depend on the molecular structure and can be explained by a simple geometric model. The surface area of each surfactant molecule on the surface of a micelle depends on a number of factors, some of which tend to increase the head group area, while others tend to decrease it. This idea of two opposite forces, introduced by Tanford [141], refers to (a) the attractive force caused by hydrophobic attraction of the hydrocarbon chain units in the hydrocarbon–water interface [142], and (b) the repulsive force between the neighbouring head groups due to the hydrophilic, steric and ionic repulsion. Both opposite forces determine the optimal area occupied by the head group. The equilibrium area per molecule at the surface is not a simple geometrical area, but an equilibrium parameter derived from thermodynamic considerations, and it can have different assumed values depending on the temperature, salt concentration, etc. [135]. Hydrophobic attraction is caused by the attempts of the hydrocarbon units to be found close to the oppositely charged part of the neighbouring surfactant molecules. This attraction force decreases the effective area occupied by the head group. The attractive free energy contribution is proportional to the surface area with the proportionality coefficient γ. The repulsive force is caused by simple steric forces, i.e., by the tendency of the hydrophilic head groups to be maximally surrounded with water molecules. In the case of ionic surfactants, additional contribution may also come from electrostatic repulsion of the head groups.

Packing parameter, p, is defined by the ratio of the volume of the hydrocarbon tail of the surfactant in the core (v_t) and the product of the optimal head group area (a_h) and of the critical chain length of the tail ($l_{c,t}$) [the effective length of the hydrocarbon tail(s) in the liquid state]:

$$p = v_t / a_h l_{c,t}, \tag{1}$$

From the thus calculated packing parameter, p, it is possible to determine the most presumable shapes of surfactant associates in a catanionic mixture [143]:

$$p = \frac{v}{al} = \frac{[x(\text{anion})(p_{\text{anion}}) + x(\text{cation})(p_{\text{cation}})]}{x(\text{anion}) + x(\text{cation})}. \tag{2}$$

The influence of geometrical parameters of surfactants on the shapes of associates is represented in Fig. 1. Additional considerable factors in the prediction of the structures of associates are the temperature, ionic strength, hydrocarbon chain length and pH. The importance of the head surface and hydrocarbon chain length was first pointed out by Tartar [144] and was theoretically interpreted by Tanford [141], Lindman [139], Israelachvili [134,138], and some other authors [145]. The influence of packing parameters on the shape of formed surfactant associates will be discussed in terms of vesicle formation.

A different approach to a better understanding of surfactants self-assembly relies on model calculations of the free energy required to form vesicles. That free energy consists of two main contributions: the size-independent work of the constituent monolayers bending and the work of the bilayer stretching determined by the planar bilayer tension [12].

2.1. Volume and critical length of the hydrocarbon chain

Hydrocarbon chain volume, v_t, refers to the volume of hydrocarbon liquid per hydrocarbon molecule. The critical chain length, $l_{c,t}$, refers to the effective length of the hydrocarbon chain in the liquid state; this semiempirical parameter defining the hydrocarbon chain length was given by Tanford [141]. The following expressions for $l_{c,t}$ and v_t for the saturated hydrocarbon chains of n hydrocarbon atoms are:

$$l_{c,t} \le l_{\max} = (0.154 + 0.1265n) \text{ nm} \tag{3}$$

and

$$v_t = (27.4 + 26.9n) \times 10^{-3} \text{ nm}^3, \tag{4}$$

where $l_{\max}$ stands for the length of the fully extended hydrocarbon chain.

The interpretation for vesicles is more complicated than that for micelles, since vesicles have an outer and an inner layer.

Fig. 2 represents the radius of the vesicle outer layer, R_0, and the outer layer thickness, t_0. For a vesicle with N_0 molecules, the outer layer volume, V_0, and the outer surface area, S_0, are given by following expressions:

$$V_0 = N_0 v_c = \frac{4}{3}\pi\left[R_0^3 - \left(R_0 - t_0\right)^3\right], \tag{5}$$

$$S_0 = 4\pi R_0^2. \tag{6}$$

The actual area per head group, a, is therefore given by

$$a = \frac{4\pi R_0^2}{N_0} = \frac{3v_c R_0^2}{[R_0^3 - (R_0 - t_0)^3]}. \tag{7}$$

The ratio of the actual area to the optimal area, a/a_0, is given by

$$\frac{a}{a_0} = 3\left(\frac{v_c}{a_0 l_c}\right)l_c \frac{R_0^2}{[R_0^3 - (R_0 - t_0)^3]}. \tag{8}$$

Eq. (8) gives the area ratio as a function of the packing parameter, the chain length, the outer radius of the vesicle, and
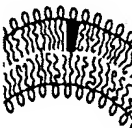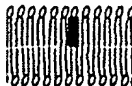
Packing parameter	Shape of the cross-section	Expected structure of associates
<1/3	cone	spherical micelle
1/3 - 1/2	truncated cone	rodlike micelle
1/2 - 1	truncated cone	flexible bilayer, vesicle
≈ 1	cylinder	planar bilayer

Fig. 1. Packing parameters and the related shapes of associates, schematically modified from Hiemenz [140].
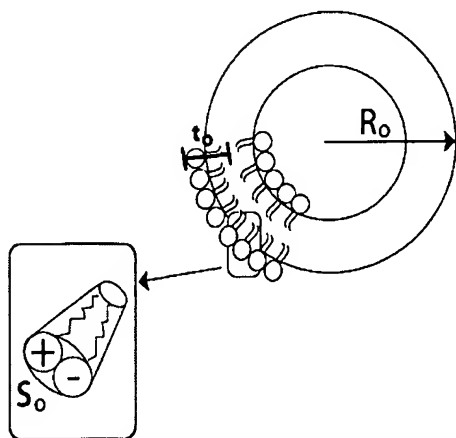
Fig. 2. Schematic presentation of the geometric parameters of the vesicle: R_0 is the radius of the vesicle outer layer; t_0 is the outer layer thickness; S_0 stands for the outer surface area.

the thickness of the outer layer. If the packing parameter and the chain length are fixed, the area ratio increases with decreasing radius, and consequently, it decreases with increasing outer layer thickness. Therefore, with a decrease of R_0, the ratio a/a_0 approaches 1. A vesicle cannot be formed without the head group area approaching the optimal value. The minimal value of R_0 is reached when the thickness of the outer layer reaches l_c. The minimal radius R_{min} refers to $t_0=l_c$. Settings $a/a_0=1$, and $t_0=l_c$ give

$$l = 3\left(\frac{v_c}{a_0 l_c}\right)l_c \frac{R_{min}^2}{[R_{min}^3 - (R_{min} - l_c)^3]}. \tag{9}$$

Eq. (9) can be solved to give

$$R_{min} = \frac{3 + \left[3\left(\frac{4v_c}{a_0 l_c} - 1\right)\right]^{\frac{1}{2}}}{6\left(1 - \frac{v_c}{a_0 l_c}\right)}. \tag{10}$$

It can be seen that the minimal vesicle size depends on the packing parameter and on the critical chain length. Formation of larger vesicles can be possible without the head group area approaching the optimal value, a_0, but such a process is entropically unfavourable.

Entropically, the formation of spherical micelles is the most favourable if the packing parameter shows the values around 1/3, since a packing parameter between 1/3 and 1/2 indicates the formation of cylindrical micelles. For P between 1/2 and 1, neither cylindrical nor spherical micelles can be formed until the optimal head group area is maintained; within that P-range, the formation of vesicles and bilayers is energetically the most favourable. When $P \cong 1$, flat bilayers are formed.

2.2. Nomenclature of vesicles: variety of vesicles

Vesicles show soft matter characteristics, fluidity, transitions of curvature, fluctuations of shapes, insolubility and incom-

pressibility. Their shapes can show deformations from closed to open objects due to the influence of shear [15].

A common case of amphiphile self-organising is the formation of bilayers with the heads oriented toward bulk water. Hydrophobic parts build the inner part of the bilayer. Planar structure represents the simplest case. By closing the bilayers, the formation of closed objects–vesicles occurs. Talking about the shape of vesicles, it has to be taken into account that vesicles are not static objects in vivo, since they are typical dynamic structures in which shape fluctuation can be considerable. With respect to the shape, size and number of bilayers, small, large and giant uni-, oligo-, or multilamellar vesicles can be distinguished [146], as schematically represented in Fig. 3.

Unilamellar vesicles consist of one bilayer, and they can show various sizes: small unilamellar vesicles, SUV, $r=4$–20 nm [142], large unilamellar vesicles, LUV, $r=50$ nm–10 μm, as well as giant unilamellar vesicles, GUV, $r>10$ μm [147]. Oligovesicular vesicles, OVV, represent the structure with small incorporated vesicles into the bigger one. Under controlled swelling, temperature and pressure changes, mechanical, electrical or magnetic shear, addition of various cosurfactants, the bilayer curvature can be changed to form altered vesicle shapes. An almost planar bilayer (having quite small curvature) can be found at LUV, defined by product $cL \ll 1$, where c is the curvature of the vesicle, and L is the maximal dimension of the amphiphilic molecule. The phase containing such unilamellar vesicles is formed from an isotropic solution, and it is denoted as L_4 phase; gels can be formed in the high-concentration region.

Giant unilamellar vesicles show a perfect spherical form with a large internal water core [148]. Fluctuating vesicle shapes
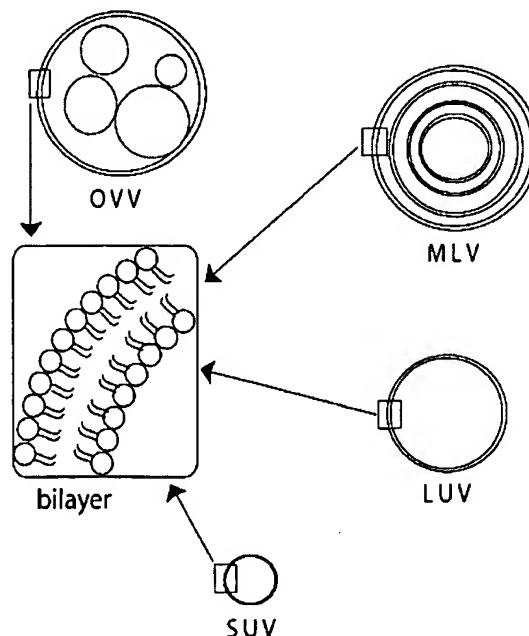

Fig. 3. Schematic presentation of vesicles structures with respect to the shape, size and number of bilayers; SUV=small unilamellar vesicle, LUV=large unilamellar vesicle, MLV=multilamellar vesicle, OVV=oligovesicular vesicle.
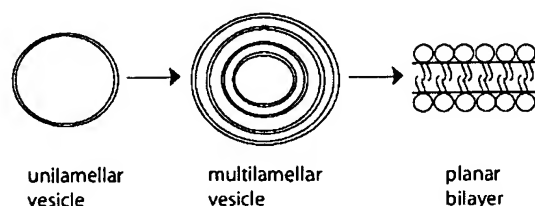
Fig. 4. Structure transitions with increasing concentration schematically represent unilamellar vesicles → multilamellar vesicles → planar bilayers.

(curvature) can be obtained by changing the externally tuned bending energy. The shapes can vary from spherical to tubular, exhibiting also examples of starfish, stomatocyte, discocyte and others [15,149–151].

Multilamellar vesicles (liposomes), MLV, built by phospholipid molecules, consist of many concentric shells exhibiting a structure similar to that of an onion, and therefore, these phases are called onion phases [152–154]. It has been observed that unilamellar vesicles are often found in diluted surfactant solutions, while MLV are usually found in more concentrated systems. Structure transitions with increasing concentrations are represented schematically in Fig. 4:

unilamellar vesicles→multilamellar vesicles→planar bilayers

Such transitions were observed by Regev for non-ionic surfactant cocodiethanolamide [65].

Oligovesicular vesicles were described by Menger [155] as the structures composed of several non-concentric vesicles inside a bigger one.

The question arises of the favourable conditions for the formation of vesicles. Following the conception of the molecular geometry, the formation of a bilayer can be expected in the case of $P > 1/2$. Such a big packing parameter requires small heads and large hydrophobic parts. This is the case of double tailed hydrocarbon amphiphiles (phospholipids), perfluoro-surfactants, and non-ionic single-tailed surfactants with small hydrophilic groups. Besides, an increase of the packing parameter of the surfactant system can be achieved by mixing with a cosurfactant, usually with medium-chain alcohols [156]. The formation of vesicles occurs in the systems with packing parameters between 1/2 and 1, while the lamellar phase is formed at $P \cong 1$. On the basis of NMR spectroscopy, and using molecular modelling, Salkar et al. have shown that the packing of polar heads in anionic/cationic mixtures plays an essential role in the formation of micelles, vesicles, or precipitate, depending on the surfactant mole ratio [157].

3. Methods of vesicles preparation

Vesicle size, polydispersity, surface potential, degree of ionisation, thermotropic phase behaviour, permeability, physical stability, and other properties depend on the preparation methods [15,158–161]. For many applications, narrow vesicle size distribution as well as high stability during a long time period is necessary [52]. Thus, the preparation method of vesicles is very important, since the formation of most vesicles requires input of external energy. Here, a brief survey of methods of vesicle preparation will be given.

If natural or synthetic long-tailed phospholipids are dispersed in aqueous solution, they form large multilamellar structures [162]. Several methods have been developed to form unilamellar vesicles from multibilayers:

- Sonication [28,29,69];
- Reverse evaporation from organic solvent [16];
- Detergent dialysis or dilution [17,18];
- Pressure/mechanical filtration [19,69,163].

Spontaneous vesiculation was observed during dispergation of oleic acid in water or in buffer solution [164].

Sonication, though a convenient method, does not produce liposomes of uniform distribution, and the results are poorly reproducible [165]. Bath sonication cannot be scaled up, while probe sonication, though potentially scaleable, is problematic owing to metal contamination, lipid degradation and generation of heat and aerosols [165].

These methods require either special equipment (sonicator, French press [166]), high-pressure extrusion [167], extrusion through Nucleopore filters [168], or additional and partial removal of nonphospholipid material (organic solvent, other surfactants) [143,169]. In many cases, the produced vesicles are unstable and tend to aggregate; they release contents and fuse into giant vesicles [149,170]. Therefore, many novel methods have been developed to form unilamellar vesicles [171–173]. The mentioned methods lead to symmetric distribution of lipids in the inner and outer leaflets of the bilayer [174]. Models of biological membranes have to include lipid asymmetry [175,176].

A classical example of phospholipid vesicles preparation is the method of sonication of aqueous lipid dispersions [30–32]. Vigorous shaking of the lipid dispersion suffices for sample homogenisation [14,23].

Methods based on dry lipid hydration are originally multistep processes (organic solvent evaporation from lipid solution, lipid drying, hydration, etc.). The so called thin-film hydration also represents a classical way of vesicles formation where a thin film is created by evaporation of amphiphile in chloroform. After the thin film contact with water, the sample becomes dissolved, forming the vesicular phase in this way [23].

Methods based on the injection of ethanol or ether lipid solution into the buffer give small vesicles [177,178]. The slow injection of chloroform [179,180] and bath- or probe-type sonication [179–181] are the most commonly used methods for preparation of small and large unilamellar vesicles. Vesicles prepared using the method of slow injection can be (meta)stable unilamellar vesicles, whereas quick injection of ethanol gives small and unstable unilamellar vesicles [182].

There are several methods based on the aqueous phase dispergation in organic solvents and on the organic solvent evaporation during vesicle formation. One of these is the reverse-evaporation method [16]. The aqueous phase is dispersed in an organic solvent (chloroform, ethyl ether, etc.) in order to form a water-in-oil emulsion by sonication of the

mixture of both phases. Then, the emulsion is placed into the evaporator under reduced pressure in order to remove the solvent. Afterwards, the aggregates are centrifuged and the supernatant is filtered to obtain unilamellar vesicles smaller than the filter pore sizes. Another method involving double emulsion is based on the formation of aqueous emulsion in chloroform and ethyl ether solutions of liposomal lipids by mechanical agitation with a shaker. Constant bubbling under nitrogen agitates the double emulsion, and unilamellar [183] or multi-lamellar vesicles [184] are formed. During the preparation, it is important to maintain the homogeneity of the suspension [185]. A modification of the reverse-phase evaporation method was recently published by Z. Zawada [186,187].

The high-pressure extrusion of lamellar phases, the so-called microfluidization technique [67,68], is another method used for vesicle preparation; shear forces destroy the lamellar surface, and the new fragments form vesicles. Using membrane filters of a chosen pore size allows the formation of monodisperse vesicles.

Extrusion/homogenisation [188,189] and microfluidization [190,191] have been shown to be scaleable. Recently, the new high-velocity jet homogeniser, used to create fine emulsions, was described [192].

Vesicle structures can be formed by block copolymers [193–197], e.g., by polystyrene-*b*-polyethylene oxide in water [198], and by polystyrene-*b*-polyacrylic acid in solvent mixtures (dioxane/THF/H$_2$O and DMF/THF/H$_2$O) [199].

Besides block copolymers, the so-called amphiphilic graft copolymers form vesicles as well. Such an example is the graft copolymer with poly-L-lysine backbone with grafted polyethylene glycol and palmitic acid. In sonication of an aqueous dispersion in the presence of cholesterol, the formation of unilamellar vesicles was observed; the size of vesicles can be controlled by the molecular weight of the copolymer [33]. Polymeric [200] and polymer-cushioned lipid vesicles [201] can also be obtained. The polymerisable amphiphiles form mixed vesicles of high stability [202,203].

Spontaneous formation of vesicles results from mixing the anionic and cationic surfactants within limited concentrations of the reacting components. Vesicles may be formed as unilamellar or multilamellar (onion-type). Typical systems that form the unilamelar vesicles are [10]:

- Mixtures of cationic and anionic surfactants (catanionic surfactants) [84,204,205];
- Mixtures of ionic surfactants and cosurfactants [34,206];
- Concentrated lamellar phases in dilution [17,18];
- Phospholipids and bile salts surfactant depletion [207].

Vesicles can be also obtained by step-by-step deposition of oppositely charged polyelectrolytes on a spherical substrate particle. After removal of the substrate particle, hollow spheres of various structures are formed. Hollow nanospheres made from polyelectrolytes are structurally very similar to the unilamellar vesicles [208].

Today, small and big unilamellar vesicles as well as multilamellar vesicles, and liposomes, can be prepared and stay stable long enough to be ready for physicochemical investigation [209].

4. Formation of vesicles

Formation of the vesicular phase requires either input of external energy or a spontaneously running process.

4.1. Induced formation of vesicles by shearing

Chemical degradation of the lipids, i.e., addition of a solvent, surfactant or salt, modifies the membrane properties. Change of temperature, exposure to UV or osmotic shock can be used to stress vesicles [210–217]. Shearing exhibits the tunability and selectivity of action for the encapsulation of drugs. It has therefore found versatile applications for vesicle preparation: LUV, d=100–400 nm are commonly produced by extrusion; the so-called onion vesicles can be obtained from lamellar phases of monocatenar surfactants by shearing in a Couette viscometer [218].

Research on the AOT/brine system [219], and on SDS/pentanol/dodecane/water [218] showed transformation of the planar lamellar phase into multilamellar vesicles using the shear field. It was also shown that the scale of the size distribution of multilamellar vesicles is related to the inverse of the square root of the shear rate [218,219]; the dynamic study of that transition involved fluctuations of the multilamellar vesicles sizes, which were investigated by DLS, polarization microscopy and conductivity measurements. It was observed that under small changes of the shear rate, the multilamellar vesicle sizes changed continuously, since the changes were discontinuous for the strong shear rate, resulting in complete destruction of the multilamellar vesicles [153]. Besides, it has been found that the shear-induced transition from lamellar phases to multilamellar vesicles is reversible [220,221]; in some special cases, it has also been observed that application of shear can induce a transition from vesicles to rod-like micelles [222,223].

Chemical reaction was used to demonstrate that vesicles in aqueous mixtures of cationic/anionic surfactants were not formed spontaneously, but the formation of vesicles in that case may be a result of shearing forces that appeared through the mixing of components [224]. Hoffmann et al. showed that it is possible to prepare metastable vesicles by shearing lamellar phases. Classical L$_\alpha$-phases with stacked bilayers were prepared without shearing forces, and they could be transferred into vesicles [225]. Similar results were obtained from a new cationic/anionic surfactant system consisting of the zwitterionic alkyldimethylamine oxide, C$_{14}$DMAO, and the anionic dihydroperfluorooctanoic acid C$_6$F$_{13}$CH$_2$COOH, DHPFOA [226].

4.2. Spontaneous formation of vesicles

In general, vesicles can be formed under various conditions if some external energy can be provided to require the thermodynamic stability of vesicles. No supply of the external energy is required for spontaneous formation of vesicles. But it has to be mentioned that it is always

necessary to apply some kind of stress in order to homogenise the system during the sample preparation. By far, the most spontaneous vesicle-forming systems reported in the literature are based on aqueous mixtures of oppositely charged amphiphiles, either with both single-tailed or with single- and double-tailed, or even with two double-tailed surfactants [51,89,99–101,105,203,205,227–237].

Classical examples of spontaneous formation of vesicles are catanionic mixtures; in such mixtures vesicles are formed simply by mixing cationic and anionic surfactants [238–242]. Spontaneous formation of vesicles from catanionic mixtures was investigated with the emphasis on the phase behaviour, structure, sizes, and stability of vesicles. Phase behaviour research of catanionic mixtures is rather complex because it constitutes a five-component system, i.e., two ionic surfactant salts, an ionic pair of amphiphiles (IPA), inorganic salt and water. Should the non-surfactant salt be removed, the number of components in IPA could be reduced to four. The most common representation of a catanionic mixture in the literature is a simplified ternary phase diagram, where the three axes of the triangle represent the anionic surfactant, the cationic surfactant and water. Usually, the results of mixing oppositely charged surfactants are micelles, vesicles and crystals [243]. Investigating the phase diagram of cationic and anionic surfactant mixtures, the lamellar phase is usually observed as the predominant phase. Mixing two surfactants with the mole fraction 50:50 resulted in the formation of either crystals or a lamellar phase in equilibrium with a highly diluted solution of counterions. The area with the excess of one component, either cationic or anionic, appears in the equilibrium between the vesicular and the lamellar phases within the solution of both components. It was observed that the precipitation always occurred in the equimolar area, and the vesicular area appeared in the excess of one of the surfactants, ensuring their stability [146]. Lindman et al. [55,56,244–246] found that the phase separation in the catanionic mixtures is similar to that observed in the mixtures of cationic and anionic polyelectrolyte and oppositely charged surfactant. The basic difference between the catanionic mixtures and cationic, anionic polyelectrolyte and surfactant are the attractive forces that exist between the aggregates, but not between the individual molecules in the polyelectrolyte mixtures.

Catanionic vesicles appeared as fascinating objects, and they have been extensively investigated using different methods, i.e., the synthesis of surfactants, theoretical modelling, physicochemical characterisation, trans-membrane properties of vesicles [247–250]. They have been intensively investigated due to their possible applications in medicine, biology and pharmacy [167,210,251–256]. Characterization of the ability of catanionic vesicles to encapsulate different types of probes is important for their application as carriers of molecules. The first published results concerning this problem came from Hargreaves and Deamer [257]. Temperature was found to be an important factor, which has to be taken into account in investigations of vesicles properties, emphasising their stability and ability of incorporation and exemption of drugs.

Investigation of the spontaneous vesicles formation was described for many systems. Dialkyl dimethylammonium surfactants, in which the halide counterions are replaced by hydroxide or acetate counterions, were investigated [258,259]. The different behaviour of the hydroxide surfactants compared to the corresponding halide surfactants is caused by the much higher affinity of hydroxide ions to water [12,107,260,261]. Removal of low-molecular-weight counterion salts of the catanionic surfactants strengthens the attractive force between the head groups of oppositely charged surfactants and reduces the head group surface area of these surfactant pairs. The repulsive interaction between head groups, and hence, also the head group area, of the surfactant molecules at the surfactant interface becomes stronger. Therefore, according to the packing parameter, planar bilayers were not formed, but curved bilayers, i.e., vesicles, were formed. Hoffmann [262] reported the dependence of vesicle formation on the counterion in the anionic surfactant, i.e., the exchange of monovalent Na^+-ion from SDS with the divalent Ca^{2+}-ion induced the process of vesicles formation in the mixtures with the zwitterionic TDMAO.

Spontaneous formation of vesicles was also described in aqueous solutions of long-chain fatty acids (oleic and linoleic), where the formation of vesicles was observed in dependence on pH [34,257,263]. New pH-induced vesicles composed of a single surfactant, sodium bis-(2-ethylhexyl) phosphate, NaDEHP, were prepared. That system can be considered as an anionic carboxylate surfactant containing the corresponding acid as cosurfactant. Much attention has been paid to pH-sensitive vesicles. Vesicles were formed by variation of the initial pH value from 6.0 to 3.0 in the NaDEHP aqueous solution. The monodispersity of vesicles was quite satisfying. Vesicle formation is a consequence of charged and uncharged surfactant molecules coexisting at certain pH values. The hydrogen bond caused the formation of dimers, which have the appropriate geometry structure to engender bilayer vesicles [264]. The size of vesicles was controlled by titration with an acid, leading to the growth of the observed vesicles [85,265].

Catanionic mixtures with single-chain surfactants are mostly investigated. Common examples of such mixtures are sodium *n*-dodecylsulfate (SDS)/*n*-dodecyl trimethyl ammonium bromide (DTAB) [32,88,266,267], cetyl trimethyl ammonium tosylate (CTAT)/sodium *n*-dodecyl benzene sulfonate (SDBS) [50,203,235–237,268–274], cetyl trimethyl ammonium bromide (CTAB)/sodium octyl sulfate (SOS) [100,101,275,276], and decyl ammonium chloride (DeAC)/sodium tetradecyl sulfate (SDeS) [87]. Precipitation within the equimolar ratio of cationic and anionic surfactants is typical of such mixtures, since in the excess of one of the surfactants, the formation of stable unilamellar vesicles occurs. It was observed that the area of the vesicular phase in the phase diagram depends on the choice of cationic as well as of the anionic surfactant. Regarding the equimolar ratio of surfactants, the area of the vesicular phase appeared as asymmetrical as the lengths of the chains of two surfactants were different. In addition, precipitation was much stronger with increasing the chain length. In the case of equal chain lengths but oppositely charged heads, precipitation

appeared even much stronger compared to the phenomena appearing in cases of a big difference in chain lengths (CTAB/ SOS) [277]. The exchange of chloride with bromide ions in the DTAB/SDBS mixture leads to the spreading of vesicular phase area [249]. These investigations indicate that counterion is an important factor in formation of the vesicular phase.

Spontaneous formation of vesicles was observed in the mixture of double-tailed didodecyl dimethyl ammonium bromide (DDAB) and single-tailed SDS [84,85,88–93]. Kondo et al. published the phase diagram of that mixture; the sizes of aggregates were determined by DLS [83]. Besides, they investigated their ability of glucose entrapment. Different areas were found in the phase diagram, i.e., homogeneous solution, liquid crystals, multiphases; within the area of a great excess of SDS, spherical micelles were found, since the vesicular phase was presented within the area of the great excess of DDAB. Between these areas, the area with micelles and vesicles appeared. Spontaneous formation of vesicles was observed in the highly diluted area of surfactants ($\omega_{surfactant} < 0.001$). Addition of DDAB to the spherical micellar solution of SDS induces growth and transition of spherical to cylindrical micelles. Marques et al. investigated the DTAB/SDBS mixture using Cryo-TEM; they determined the stability and sizes of vesicles [84–86]. Vesicles in the aqueous DDAB/DTAC mixture within the high-dilution region were most easily formed at a considerable excess of DTAC after a gentle mixing. The vesicles were polydispersed with two main populations around $d = 40$–50 nm and $d = 500$–600 nm [99]. Also, intact vesicles, vesicles with ruptured membranes, small bilayer disks, and globular micelles were visualized by Cryo-TEM.

The much investigated catanionic mixture of both single-tailed anionic SDBS and cationic CTAT, was described in many papers [50,203,249,250,277,278]. Kaler et al. determined the phase diagram of the above-mentioned mixture [50]. The area of positively charged, spontaneously formed vesicles appeared with a great excess of cationic surfactant. In the region with coexisting micelles and vesicles, an increase in the molar fraction of cationic surfactant caused the appearance of the cylindrical micelles region. They investigated the influence of the electrolyte on the stability of spontaneously formed vesicles [203], and observed the long-period stability (at least 1 year) of positively or negatively charged vesicles (in dependence on the surfactant in excess) and their ability of glucose entrapment. Walker et al. [277] investigated aqueous mixtures of cationic CTAT and anionic SDBS, in which spontaneous formation of equilibrium "catanionic" vesicles was observed whose charge depends on the mole fraction of each surfactant. The short-range forces of the specific recognition interaction enabled the aggregation control via electrostatic phenomena. These results suggested that electrostatic interactions were responsible for the stability of the spontaneously formed vesicles. Spontaneous formation of vesicles is accompanied by the transition of micellar aggregates into the vesicular phase. In many mixtures, coexistence of micellar and vesicular phases was observed [249,254], e.g., in the catanionic mixture of DTAC/SDBS; besides, continuous transition of spherical micelles–cylindrical micelles–unilamellar vesicles was also found.

Determination of the structure and size of spontaneously formed vesicles showed that besides small unilamellar vesicles (10–50 nm), large vesicles (50–500 nm), multilamellar vesicles (1–50 µm), and ultra-small unilamellar vesicles (5–10 nm), could be found. The last mentioned ultra-small unilamellar vesicles, USUV, with coexisting cylindrical micelles were observed within the catanionic mixture SDS/DDAB [279]. The appearance of USUV amounting to 2.5–5 nm was observed recently in the systems of SDS/DDAB [84,280], TDMAO/HCl/ hexanol [281], and triton X-100/CPyCl/1-octanol [109,282]. The formation of such vesicles occurred when mixing of ionic and non-ionic surfactants in high dilutions where the volume fraction of surfactants did not exceed 3%. In vesicles of such small dimensions, the high curvature of a bilayer requires strong electrostatic interactions within the high dilution. It was observed that the addition of salt to USUV systems caused their disappearance. Besides, a small addition of salt to the system TDMAO/HCl ensured no formation of USUV, but only formation of big MLV [281]. In the phase diagram of the ternary surfactant system TDMAO/HCl/1-hexanol/water, with increasing of cosurfactant concentration, the formation of one L_1-phase, two L_α-phases (a vesicle phase $L_{\alpha 1}$ and a stacked bilayer phase $L_{\alpha h}$), and one L_3-phase, separated by the corresponding two-phase regions L_1/L_α and L_α/L_3, was observed. At surfactant concentrations lower than 80 mM, the L_1^*-phase borders directly on the L_1-phase. The phase L_1^* contains SUV of about 10 nm in size, and some large multilamellar vesicles with diameters up to 500 nm. Phase transition between the L_1-phase and the L_1^*-phase was detected by electric conductivity and rheological measurements [281].

A new monodisperse vesicular system was found recently; vesicles were formed in the aqueous mixtures of cationic tri-(N-dodecyl dimethyl hydroxypropyl ammonium chloride) phosphate, PTA, and AOT, which was supported by negative-staining TEM and DLS [95]. Vesicles diameters increase with the total surfactant concentration. Tubular microstructures, vesicle fusion, and vesicle-tubular microstructure transition have been also observed. The vesicle formation mechanism is discussed from the viewpoint of molecular geometry, conformation, and the interaction between surfactant molecules.

By designing chemical reactions within extremely dilute catanionic aqueous mixtures of single-tailed surfactants in order to get spontaneously formed vesicles without shear forces, thermodynamic stable mixtures were studied [283]. This was achieved if one of the components was produced by chemical reaction and not by the mixing of components.

Vesicles were also observed within the diluted range of the phase diagrams of binary systems of non-ionic single-chain surfactant ($C_{12}E_4$)/water, where the vesicular phase is denoted as L_α^+ [284,285]; vesicle formation is strongly temperature dependent. Such vesicles can be stabilised by different factors, e.g., by adding additives (cholesterol) [286], by mixing with ionic surfactant [287], by adding a cosurfactant (benzyl alcohol) [288]. Similar phase behaviour was found in ethoxylated perfluorocarbon alcohols, which form unilamellar vesicles within dilute areas of the phase diagram [289].

Addition of a cosurfactant (amine or aliphatic alcohol) can facilitate the formation of vesicles in various systems [32,290–304], in which formation of large multilamellar vesicles was found: these vesicles can be easily observed by polarisation microscopy [65,294,305]. Formation of vesicles can also be induced by the addition of amphiphiles with polymeric hydrophilic groups (such as stearyl alcohol monoether with a PEO group) to the surfactant solution [160]. Such a modified lipid can be used to increase the stability of phospholipid vesicles [306].

Recently, vesicles were prepared by mixing TTAOH and fatty acids (decanoic acid, lauric acid, myristic acid, and palmitic acid) at concentrated salt-free cationic/anionic surfactant concentrations [307].

Spontaneous formation of vesicles can also occur within non-aqueous systems, e.g., sucrose monoalcanoate and hexaethyleneglycol hexadecyl ether in decane [56] as well as in the organic solvents with long-tailed bischiff bases and their organometallic complexes [308].

Highly important groups of attractive intermolecular interactions that reduce monomer mobility and, therefore, promote the formation of stable bilayers and vesicles are hydrogen bonds, the metal ion coordination, and the electrostatic attraction. The directional order within these interactions decreases, from one-directional hydrogen bonds to multi-directional metal ions (depending on the respective coordination number) to non-directional or isotropic electrostatic attraction [309].

5. Methods and techniques of structure and properties determination

Starting with the determination of phase diagrams, well-separated areas of micelles and vesicles with continuous transition from micellar to vesicular phase, as well as coexistence of micelles and vesicles in the diluted amphiphile solution, were found [97,107,238,252,254]. The choice of methods for the investigation of phase transitions will depend on the thermodynamic stability of the vesicular phase. According to the Gibbs' phase rule and phase transition, the thermodynamic equilibrium is an important issue [57]. In the systems with vesicles that retain stability long enough, the first identification of the phases can be done by visual methods, usually polarisation light microscopy [83], freeze fracture transmission electron microscopy, FF-TEM, [50,102,269,277], and Cryo-TEM, [84,86,251,268,292,310]. Photomicrographs represent the first evidence of vesicle formation in the systems, undoubtedly proving the presence of an inner hollow sphere surrounded by a bilayer or a multilayer. An example of vesicles is shown in Fig. 5 [106].

The most used techniques for the investigation of shapes, sizes, and phase transitions are NMR-self diffusion, time-resolved fluorescence quenching, small-angle neutron scattering, SANS, and the other scattering techniques, i.e., SAXS, DLS. In addition, rheology techniques play an important role, since the phases can be distinguished owing to different properties, i.e., fluidity, density, and viscosity.
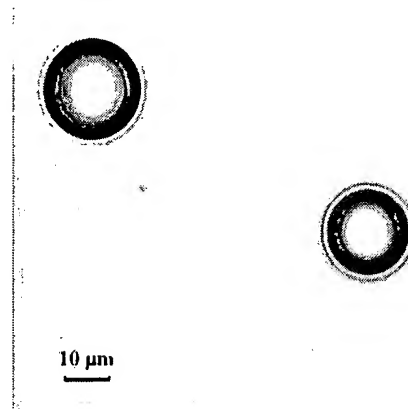

Fig. 5. Optical micrograph of two vesicles formed in the aqueous DDAB solution, $\omega = 0.0075$, at 30 °C. Bar: 10 μm.

5.1. Visual observation of the colloid systems

Techniques for direct observation of colloids, optical visualisation techniques, require an acceptable difference between the refractive index of the particles and that of the surrounding medium; this is known as contrast. Contrast is dependent on the used technique as well as on the radiation applied. Using DLS, contrast is due to the difference between the refractive indices of the particles and the surrounding medium. Using SAXS, contrast represents the difference of the electron density between the particles and the surroundings. In the classical neutron scattering, contrast represents the difference in the interaction between the neutrons and the atomic nuclei.

5.1.1. Optical microscopy

The main characteristics of optical microscopy are magnification and the limit of resolution (resolving power). Magnification determines the size of an image, and the resolving power identifies the amount of distinguishable details. The light beam is always diffracted at the edges of an object producing a set of images of the edge, known as the diffraction pattern. Human eye receives the diffracted light from an object and the image of the object is constructed in the eye. Diffracted light contains sufficient information to assemble an image; any light not incorporated into the image will result in a loss of details in the image [311].

Diffraction radiation is represented by the Bragg equation, and it also represents the relation for all diffraction phenomena.

$$d\sin\theta = \frac{\lambda}{n}, \tag{11}$$

where λ is the wavelength of radiation within the medium, n is the refractive index of the medium, d is the distance between pinholes, and θ is the angle of an incident beam. The resolving power of a microscope, when the angle subtended by the microscope is 2θ, is defined as the magnitude of the separation between objects that is required to produce

different images. Therefore, the resolving power is identical to the distance, d, and it is estimated to be

$$d = \frac{\lambda}{2n \sin \theta}.$$ (12)

Eq. (12) indicates that the resolving power is decreased by increasing θ, or by decreasing the ratio λ/n. The subtended angle 2θ is increased by increasing the lens diameter and by decreasing the distance between the object and the lens. The ratio λ/n may be decreased by decreasing λ or by increasing n. Although shorter wavelengths improve the resolving power, visible light is almost always used in microscopy, primarily because of the absorption of shorter wavelengths by glass.

In Fig. 6, an optical micrograph represents an example of an oligovesicular vesicle formed in the catanionic mixture DDAB/SDBS/H$_2$O [106].

In Fig. 7, imaging of a multilamellar vesicle, obtained by digital light microscopy of the system from Fig. 6, is shown.

5.1.2. Electron microscopy

The best prospect of extending the range of microscopy lies in the extension by orders of magnitude of the wavelength used to produce the image. In an electron microscope [311], an electron beam has a role in producing an image. Electron beam is produced by a hot filament, accelerated by an electron gun, and focused by electric and/or magnetic fields from electromagnets acting like lenses in the light microscope. The technique is known as the transmission electron microscopy (TEM).

The solving power of a conventional electron microscope is generally about 1 nm. The intensity of the transmitted electron beam through the specimen under observation depends on the thickness of the sample and the concentration of atoms in the sample. The most common way of overcoming a very low contrast is shadow casting.

Complementary to scattering methods, Cryo-TEM allows visualisation of many of the microstructures that are formed by
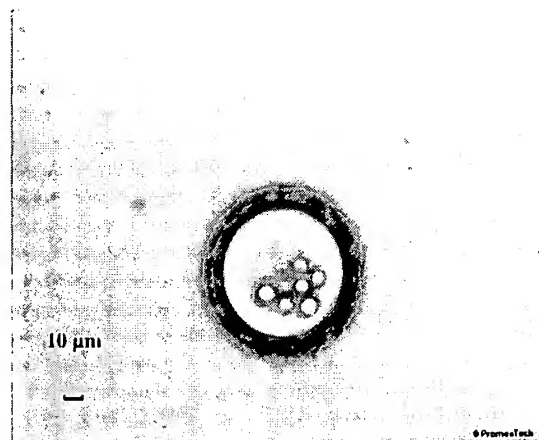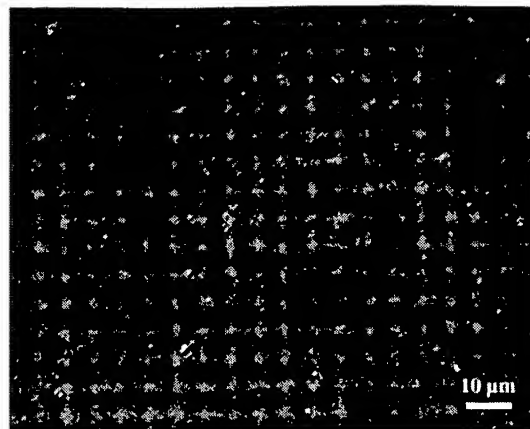
Fig. 7. The DLM image indicates wide size range of multilamellar vesicles, up to several micrometers in size, formed in the catanionic mixture DDAB/SDBS/H$_2$O, ω_{tot}=0.0075, x(SDBS)=0.6. The sample was provided by courtesy of Y. Talmon.

self-assembly of amphiphilic molecules [312], i.e., simple surfactants, lipids, or polymers. An important feature of that method is the examination of samples without staining or dehydration, which is achieved by capturing the structures within thin aqueous films, subsequently vitrified at liquid nitrogen temperatures.

Cryo-TEM provides information about the size distribution of equilibrium multi-aggregates. Jung et al. observed the equilibrium of novel bilayer cylinders with hemispherical end caps, and open flat discs coexisting with spherical unilamellar vesicles in the mixtures of CTAB/sodium octyl sulphonate (FC$_7$) catanionic systems by Cryo-TEM [313].

The origins of the stability of different catanionic vesicles formed by CTAB/FC$_7$ catanionic mixed surfactants have been analyzed by Cryo-TEM and SANS [314].

Recently, a Cryo-TEM study was performed to demonstrate the possible formation of silicate–surfactant vesicles during the course of the reaction where the lamellar phase dominates [315].

FF-TEM analyses of the vesicle suspensions were carried out in the mixtures of decanoic acid and sodium decanoate, in which micelles and vesicles are always present along with nonmicellised or nonvesiculised decanoate. Regions within which vesicles exist were identified on the basis of the FF-TEM analysis and other complementary techniques, such as differential scanning calorimetry, DSC, and titration curve measurements [254].

Super-thermostability of the vesicles in mixed systems was investigated recently [97]. Small spherical vesicles, formed in bolaamphiphile/oppositely charged conventional surfactant mixed systems were revealed by FF-TEM. It was shown that the variation of the structure of the hydrophobic chain of bolaamphiphiles has a strong influence on the vesicle formation ability. Vesicles were found in a single system of a carboxylate bolaamphiphile, which was attributed to the hydrolysis of the bolaamphiphile. The results showed that bolaamphiphiles spanned through the vesicle membranes.

Precipitate of the equimolar catanionic surfactant mixtures in the excess and salt-free catanionic surfactant solutions was

Fig. 6. Optical micrograph of the oligovesicular vesicle formed in the catanionic mixture DDAB/SDBS/H$_2$O, ω_{tot}=0.003, x(SDBS)=0.4, at 30 °C. Bar: 10 μm.

characterised by polarization microscopy, by differential interference contrast microscopy, DIC, and by FF-TEM [107].

The aggregation behaviour and microstructures of cationic surfactants and hydroxy-naphthoate were studied using FF-TEM and by rheological measurements [316].

5.2. Methods of electromagnetic radiation scattering

Different scattering techniques are used as complementary procedures in colloid chemistry research. Using SAXS, particle sizes within the range from 1 to 100 nm can be determined. In the range of particle sizes from 100 nm up to several micrometers, elastic light scattering, ELS, can be applied. DLS can be used for particle sizing and shape analysis in a much wider range (about three decades) but allowing a lower resolution [317,318]. The whole range of elastic scattering, ES, is described by three theories, Rayleigh–Debye–Gans', Lorenz–Mie theory and Fraunhofers diffraction [317,319]. Brownian motion of particles in the solution causes the Doppler effect. A spectrum of scattered light contains frequency components that incident light does not contain. Based on that effect, such light scattering is named quasi-elastic scattering, QELS [320,321].

The validity range of a particular scattering method is determined by the size of the object in relation to the wavelength, λ, by the relative refraction index (known as optical contrast), $m = n_{particle}/n_{solvent}$, as well as from the phase (phase shift) of the incident beam through the scattering object, $2ka(m-1)$, where $k = 2\pi/\lambda$.

Ranges of dimensions observed by different scattering methods are represented in Fig. 8.

The condition for phase shift, $2ka(m-1) \ll 1$, has to be fulfilled, and it is fulfilled in the case when the particles are much smaller than the light wavelength, i.e., when the relative refractive index shows the value amounting approximately to 1 ($m \to 1$). Interference of the scattered light depends on each volume unit from which electromagnetic radiation comes out, and it also depends on the mutual space arrangements of the volume units. The intra-particle interferences will be diminished with the decreasing of particle sizes. The Rayleigh–Debye–Gans theory is also valid for

Fig. 8. Ranges of applicability of the scattering methods. Reproduced from H. Brumberger, "Modern Aspects of Small Angle Scattering", Kluwer Academic Publishers, London, 1995, p. 112. With kind permission of Prof. Otto Glatter. With kind permission of Springer Science and Business Media.

SAXS and SANS. When the frequency of a radiation is strong, the bonding electrons scatter the radiation as free electrons, and this also happens by SAXS.

5.2.1. Time dependence of scattering intensity

Time behaviour of scattering is influenced by particle motion, and it is shown in fluctuations of scattering intensity. Brownian motion of particles in solution caused the phenomenon named the Doppler shift of scattered light. The spectrum of scattered light contains the vibration components that the incident light did not possess. The autocorrelation function, $G(t)$, and the power spectrum, $P(\omega)$, are interconnected by the Fourier transformation [322]:

$$P(\omega) = \frac{1}{2}\pi \int_{-\infty}^{\infty} G(t)e^{i\omega t}dt \overset{FT}{\leftrightarrow} G(t) = \int_{-\infty}^{\infty} P(\omega)e^{-i\omega t}d\omega, \qquad (13)$$

where t is the time, and ω is the frequency of the light.

5.2.2. Dynamic light scattering

The technique that provides information about the Brownian motion of particles on the basis of the intensity of scattered light fluctuation analysis is called DLS, QELS, photon correlation spectroscopy, PCS, and laser Doppler spectroscopy [323–328]. The principles of DLS have been described in the book edited by Pecora [329] and by Brown [330], and the special problems of particle sizing with this technique have been discussed in the book edited by Dahneke [331]. An extensive summary of theoretical treatments, including historical aspects, experimental methods for determination of particle size and shape, and measurement of refractive index have been given in the review by Jones [332].

When particles move in the motion direction of the scattering vector, a light frequency shift happens, Δv, (Doppler Effect); the frequency shift is dependent on the scalar product of the scattering vector and the rate vector.

The assumption is that the system is a suspension of monodisperse particles. The diffusion process in such system corresponds to the varying velocity of particles in different directions, and only the components in the direction of scattering vector contribute to the frequency spectrum. The appropriate signal is a stochastic one, i.e., there exists no fixed amplitude–frequency–phase relation. One of the methods to evaluate such signal is the analysis in the time domain, i.e., the calculation of the time autocorrelation function of the scattered intensity:

$$G_2(\tau) = \frac{1}{T}\int_0^T I(t)I(t+\tau)dt \qquad (14)$$

The correlation function, $G_2(t)$, for the system of monodisperse particles is an exponentially decaying function on a constant background which contains all high-frequency experimentally unresolved terms. The intensity correlation function of a monodisperse system consists of three terms,
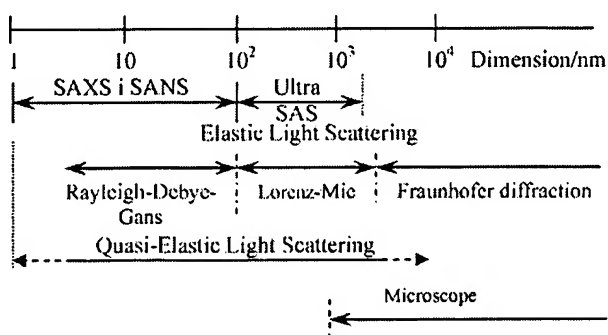
i.e., the constant baseline, the exponentially decaying signal and the shot noise term (a delta function at $t=0$):

$$G_2(t) = A[1 + C_i e^{-2Dh^2 t}] + C\delta(t) \tag{15}$$

where h is the length of the scattering vector, D is the diffusion constant, and C_i is the intercept with the theoretical maximum value of 1. The decay constant in the exponential function is

$$\tau = \frac{1}{Dh^2} = \frac{1}{\Gamma} \tag{16}$$

The correlation function of the electrical field, $G_1(t)$, is connected with the correlation function of the scattering intensity, $G_2(t)$, by the relation

$$G_2(t) = A[1 + C_i(G_1(t))^2] \tag{17}$$

The diffusion constant D determined from DLS experiments is related to a hydrodynamic radius, R_H, by the Stokes–Einstein relation

$$D = \frac{k_B T}{6\pi\eta R_H} \tag{18}$$

where k_B is the Boltzmann constant, T is the temperature, and η is the viscosity of the solvent. This equation clearly shows that the diffusion velocity of the considered particle is the same to the velocity of the sphere with the radius R_H, without any information about the shape of the particle. By introduction of the equation for decay time into the above equation, and by neglecting the delta function at $t=0$, it can be shown that the correlation function of the scattering intensity, $G_2(t)$, is equal to

$$G_2(t) = A\left[1 + C_i e^{-\frac{2t}{\tau}}\right] = A\left[1 + C_i e^{-2\Gamma t}\right], \tag{19}$$

and the decay time, τ, is directly related to the hydrodynamic radius R_H:

$$\tau = \frac{3}{8\pi} \frac{\eta\lambda^2}{k_B T} \frac{R_H}{\sin^2(\theta/2)}. \tag{20}$$

The decay time is larger with the R_H increase, i.e., the correlation function, $G_2(t)$, shows a rapid decrease for small particles. For monodispersed systems, the size of the particles, i.e., hydrodynamic radius can be estimated directly from the correlation function.

In the system of polydisperse particles of different shapes and sizes, the correlation function of the electrical field, $G_1(t)$, is represented by the sum over all exponentials describing the different particles. In the case of a continuous size distribution, the field correlation function is represented by the integral

$$G_1(t) = \int_{\Gamma_{min}}^{\Gamma_{max}} G(\Gamma)e^{-\Gamma t}d\Gamma, \tag{21}$$

or with

$$G_1(t) = \int_{\Gamma_{min}}^{\Gamma_{max}} D(\tau)W(\tau)e^{-t}d\tau, \tag{22}$$

where $D(\tau)$ is weighting factor, and it is presented by

$$W(\tau) = 1 \text{ for intensity distribution } D_i \tag{23}$$

$$W(\tau) = \tau^3 \text{ for volume distribution } D_v \tag{24}$$

$$W(\tau) = \tau^6 \text{ for number distribution } D_n \tag{25}$$

There are three methods for evaluation of data from polydisperse systems. The first method for the determination of the correct distribution function, $D(\tau)$, is the inverse Laplace transformation of Eqs. (21) and (22) [333]. The second method is the simplest method known under the name cumulant method. If the constant baseline is substructed, the correlation function of the monodisperse system show a linear behaviour in a semi-logarithmic plot of $\ln[G(t)]$ vs. t, and any deviation from linearity is due to the polydispersity of the system. It can be written as

$$\ln[G_1(t)] = K_0 - K_1 t + \frac{K_2 t^2}{2!} - \frac{K_3 t^3}{3!} + -... \tag{26}$$

For the monodisperse system, K_0 is an amplitude factor, $K_1 = Dh^2 = \Gamma$, and all further K_i are zero. For a polydisperse system,

$$K_1 = \langle\Gamma\rangle, \tag{27}$$

$$K_2 = \langle(\Gamma - \langle\Gamma\rangle)^2\rangle. \tag{28}$$

It can be seen that K_1 is the mean (z-average) of the Γ-distribution, and K_2 is the variance of the Γ-distribution [334]. The polydispersity index, V, is the ratio of K_2 and the square of K_1,

$$V = \frac{K_2}{K_1^2} \tag{29}$$

The third method for the evaluation of the DLS data is the fast and simple method to realize strong polydispersity. If either log $[G_1(t)]$ vs. $\log(t)$ or $G_1(t)$ vs. $\log(t)$ are plotted, that plot for the monodisperse system presents a sigmoidal curve with one step centered at a position $t=\tau$. In the case of a bimodal distribution, two steps can be seen if the decay constants differ at least by one decade. If two decay constants differ by a factor less than 10, two steps melt into one broader step.

The transition from vesicles to micelles by adding octane into the dodecyl-pyridinium chloride (DPCl)/sodium laurate (SL), and DTAB/SL aqueous two-phase systems was studied. The two-phase systems were transformed into single-phase isotropic solutions by the addition of a certain amount of octane. DLS results demonstrated the decrease of large aggregates (vesicles) and the increase of the small aggregates (spherical micelles) upon octane addition [335].

Microstructures formed by mixtures of two polymerisable surfactants, cationic methacryloyloxyundecyl trimethylammonium bromide and anionic sodium 4-(ω-methacryloyloxyundecyl)oxy benzenesulphonate, in aqueous solutions including

stable vesicles were investigated. Both native and polymerised vesicles were characterised using DLS and SLS, SANS, and Cryo-TEM [203].

DLS is a good method for investigating the dynamics of vesicle formation and their growth. An example of such investigation was recently reported by Shioi et al. [336]. They investigated the mixing of CTAB and SOS surfactant solutions using SLS and DLS. Sizes of the initial vesicles correlated well with the equilibrium sizes determined after 2 months. The results were described by the two-stage model in which the initial nonequilibrium vesicles were generated rapidly following the mixing of the surfactant solutions, and the subsequent vesicle growth was demonstrated by slower vesicle fusion.

Heterogeneous multilamellar vesicle sizes, as well as their polydispersity, can easily be determined by DLS measurements as a complementary technique to electron microscopy or SANS. Such determination was reported by Namani et al. [254] in the mixtures of decanoic acid and sodium decanoate in aqueous solutions.

Recently, using DLS and TEM, Taneva et al. [337] showed that dimers of phosphocholine cytidylyltransferase (CCT) can cross-bridge separate vesicles to promote vesicle aggregation. The vesicles contained either class I activators (anionic phospholipids) or the less potent class II activators, which favor nonlamellar phase formation. CCT increased the apparent hydrodynamic radius and polydispersity of the anionic phospholipid vesicles even at low CCT concentrations corresponding to only one or two dimers per vesicle. Electron micrographs of negatively stained phosphatidylglycerol (PG) vesicles confirmed CCT-mediated vesicle aggregation.

5.2.3. Small-angle X-ray scattering

Using SAXS, it is possible to investigate monodisperse as well as polydisperse systems. In monodisperse systems, sizes, shapes, and inner structures of particles can be determined. Meanwhile, monodispersity cannot be deduced only from SAXS data, but it has to be assumed, or checked by other independent methods. For polydisperse systems, the size distribution can be evaluated under the assumption of a certain shape of the particle. All these considerations can be strictly applied to highly diluted systems where the interparticle distances are much larger than their dimensions.

In the case of semi-dilute systems, the SAXS result is influenced by particle structures and their spatial arrangement. The scattering curve of spherical particles is the product of the particle scattering function, form factor, and of the interparticle interference function, structure factor. If the form factor of the particle is known, it is possible to evaluate the information about the radial distribution of these particles from the structure factor.

SAXS uses radiation with the wavelength in the range of 10^{-1} nm to 10^0 nm, depending on the specific problem, and on the used source of radiation. This range is also valid for SANS. While neutrons interact with the nuclei of the atoms, X-rays interact with the electrons. The scattering efficiency increases linearly with the increasing atom number. The wavelength and the scattering efficiency limit the range of SAXS experiments to

the systems whose sizes range from a few nanometers up to about 100 nm.

Particles in the size range from 100 nm up to several micrometers can be investigated by SLS. Particles exceeding that limit can be investigated by optical microscopy or by the Fraunhofer diffraction. Electron microscopy represents a complementary method to all the mentioned scattering methods. It has a considerable advantage in the real picture of systems with high resolution. Physical principles of scattering are the same for SAXS and for the wide-angle diffraction of X-rays at large angles; this is used in crystallography. The electric field of the incoming wave induces dipole oscillations within the atoms. The energy of X-rays is high enough to cause excitation of all electrons. The accelerated charges generate secondary waves, which at large distances increase the scattering amplitude. All secondary waves have the same frequency, but they may have different phases, caused by different path lengths. Due to high frequency, only the scattering intensity and the scattering dependence on the scattering angle can be detected. The angle-dependent scattering amplitude is related to the electron-density distribution of the scatterer by the Fourier transformation. All this holds for both wide-angle diffraction and small-angle X-ray scattering (SAXS). There is a periodic arrangement of identical scattering centers (particles) in the case of the wide-angle diffraction, i.e., the scattering medium is periodic in all three dimensions with a large number of repetitions, whereas in SAXS, these particles are not ordered periodically. The particles are embedded with arbitrary orientation and with irregular distances in a matrix like water. The scattering centers are limited in size, nonoriented and unperiodic, but the number of particles is high and they can be assumed to be identical like in crystallography. The Fourier transform of an unperiodic limited structure corresponds with a Fourier integral. In mathematical terms, it is the expansion of an unperiodic function by a periodic function system [323,338]. The difference between crystallography and SAXS are equivalent to the difference between a Fourier series and a Fourier integral. This is, in principle, the way of scattering working. In SAXS, a continuous angle-dependent scattering intensity at discrete points instead of sharp, point-like spots is measured. Another important point is that in SAXS there is a linear increase of the signal (scattered intensity) with the number of particles in the measuring volume since intensities are adding due to the incoherence of the scattered waves from separated particles. Besides, there is a loss of information in SAXS experiments caused by the averaging over all orientations in space. The three-dimensional structure is represented by an one-dimensional function, i.e., by the dependence of the scattered intensity on the scattering angle.

The electron density, $\rho(r)$, is the number of electrons per unit volume at the position **r**. A volume element dV at **r** contains $\rho(\mathbf{r})dV$ electrons. The scattering amplitude of the whole irradiated volume, V, is given by

$$A(\mathbf{h}) = \int \int \int \rho(r) e^{-i\mathbf{h}\mathbf{r}} dV, \qquad (30)$$

where h is the scattering vector that bisects the angle between the scattered beam and the incident beam, and has the length

$h = \left(\frac{4\pi}{\lambda}\right)\sin\theta$, where 2θ is the scattering angle, e.g., the angle between two unit vectors defining the direction of the incident and scattered beam. The intensity, $I(h)$, of the complex amplitude, $A(h)$, is given by the product of the amplitude and its complex conjugate, A^*

$$I(h) = A(h)A(h)^* = \int \int \int \tilde{\rho}^2(r)e^{-ihr}dV \qquad (31)$$

where $\tilde{\rho}^2(r)$ is the convolution square [339]. Until now, it was observed that the scattering process of a particle is in fixed orientation in a vacuum. In many cases of SAXS, the scatterers (particles) are statistically isotropic and there is no correlation between points in great spatial distance. Furthermore, the scatterers are embedded in a matrix which presents a homogeneous medium with the electron density ρ_0. For particles in solution the electron density should be replaced by the difference of electron density of particle and the medium, $\Delta\rho=\rho-\rho_0$, in Eqs. (30) and (31).

The average over all orientations $\langle\ \rangle$ leads to [340]

$$\langle e^{-ihr}\rangle = \frac{\sin(hr)}{hr}, \qquad (32)$$

and Eq. (31) reduces to the form

$$I(h) = 4\pi \int_0^\infty r^2 \Delta\tilde{\rho}^2(r)\frac{\sin(hr)}{hr}dr. \qquad (33)$$

Introduction the pair distance distribution function $p(r)$ [341]

$$p(r) = r^2\Delta\tilde{\rho}^2(r) = r^2 V\gamma(r) \qquad (34)$$

in Eq. (33) leads to

$$I(h) = 4\pi \int_0^\infty p(r)\frac{\sin(hr)}{hr}dr; \qquad (35)$$

$\gamma(r)$ is the correlation function [342], and by light scattering

$$\gamma(r) = \langle\Delta\alpha(r)^*\Delta\alpha(-r)\rangle, \qquad (36)$$

where $\Delta\alpha(r)$ is the change in the polarisability of particles.

5.2.4. The scattering problem and the inverse scattering problem

The issue is the scatterer of the known size, shape, and three-dimensional structure; the corresponding distance distribution function, $p(r)$, as well as the scattering function, $I(h)$ can be calculated. This is the scattering problem and it can be solved. The inverse scattering problem is an attempt to determine the size, shape and internal structure of the particle from the measured scattering intensities.

Solution of the inverse scattering problem is in the calculation of the distance distribution function, $p(r)$.

$$p(r) = \frac{1}{2\pi^2}\int_0^\infty I(h)hr\sin(hr)dh \qquad (37)$$

The $p(r)$ function gives the number of difference electron pairs with a mutual distance between r and $(r+dr)$ within the particle. For homogeneous particles (constant electron density), this function has a simple and clear geometrical definition. If the particle is subdivided into a very large number of identical small volume elements, than the $p(r)$ is proportional to the number of lines with a length between r and $(r+dr)$ which are found in the combination of any volume element i with any other volume element k of the particle. Therefore, $p(r)$ is a distance histogram of the particle. There is no information about the orientation of these lines in $p(r)$, because of the spatial averaging. In the case of inhomogeneous particles, each line is weighted with the product of the number of difference electrons, $\Delta\rho dV$, of the volume elements. This can lead to negative contributions to the $p(r)$. From Eq. (35) it can be seen that every distance r gives a $\sin(hr)/(hr)$ contribution with the weight $p(r)$ to the total scattering intensity. $I(h)$ and $p(r)$ contain the same information, but it is easier to analyse the data in terms of the distance than in terms of $\sin(hr)/(hr)$ contributions.

Methods of first-order approximation provide solutions to the inverse scattering problems in order to get the first model using minimum a priori information about the system. To check that model, the scattering problem has to be solved. The resulting theoretical model of the function can be then compared with experimental data, and if necessary, modifications of the model have to be performed from deviations. After several iterations, the final model was obtained. The iterations were done by changing the parameters. It should be noticed that it is possible to find different models that fit the data within their statistical accuracy. In order to reduce this ambiguity, it is necessary to have additional independent information from other experiments Wrong models can be rejected when their scattering functions differ significantly from the experimental data.

By SAXS it is possible to study monodisperse and polydisperse systems. In the case of monodisperse systems it is possible to determine size, shape and under certain conditions the internal structure. Monodispersity must be assumed or checked by independent methods. Independent a priori information is necessary to make such a decision. For polydisperse systems, a size distribution can be evaluated under the assumption of a certain shape of the particles. All these statements are strictly valid for highly diluted systems where the interparticle distances are much larger than the particle dimensions. In the semi-dilute systems the result of the SAXS experiment is influenced by the structure of the particles and by their spatial arrangement. In the case of spherical particles the scattering curve is a product of the particle scattering function (form factor) and of the interparticle interference function (structure factor) [323]. The basic relation between the scattered intensity and the form factor for reasonably monodisperse globular particles is given by

$$I(h) = nP(h)S(h) \qquad (38)$$

where n is the number density of particles (cm^{-3}), $S(h)$ is the structure factor, and $P(h)$ is the form factor, sometimes called the interparticle scattering function. $P(h)$ of a colloidal sample is the scattering of one independent particle (independent meaning

interpenetrable and without interaction). $P(h)$ units are in square centimeters, allowing absolute scaling of the scattered intensity in cm^{-1} and has analytical expressions for most shapes of particles. Structure factor, $S(h)$, usually called the intermediate scattering function, is a numeric multiplicative term reflecting the coherent interference between scattering generated by neighbouring colloidal particles. The maximum of $S(h)$ reflects the most probable interparticle distance. Dilution procedures are meant to obtain the "dilute solution" condition, which is $S(h) \approx 1$ at any h value [327].

5.2.5. Monodisperse systems

Monodisperse systems contain the same particle size, shape, and internal structure. These characteristics are usually found in the case of biological macromolecules in solution. It is supposed that these solutions are at infinite dilution; therefore, experiments are performed as a series of scattering functions at different concentrations, and the extrapolations of these data to the zero concentration, c_0, give the value at infinite dilution.

Particles can be roughly described by some parameters extracted from the scattering function [329,327,344,346]. More information about the particle shape and structure can be found by detailed analyses of the scattering function. In general, it is much simpler to discuss features of the distance distribution function, $p(r)$, than of the scattering function, but meanwhile, some characteristics like symmetry give more pronounced effects in the reciprocal space.

5.2.5.1. Homogeneous particles

5.2.5.1.1. Globular particles. The most trivial shape is a sphere. The analytical expressions for the scattering intensity

$$I(h) = \left(3 \frac{\sin(hr) - (hr)\cos(hr)}{(hr)^3} \right)^2, \tag{39}$$

and for the $p(r)$ function [343]

$$p(r) = 12x^2 \left(2 - 3x + x^3 \right) \quad x = \frac{r}{2R} \leq 1 \tag{40}$$

where R is the radius of the sphere. The $p(r)$ function of the sphere has a maximum near $r = R = D/2$ and drops to zero like every $p(r)$ at $r = D$ where D is the maximum dimension of the particle, meaning diameter.

5.2.5.1.2. Rodlike particles. Long cylinders, prisms, etc., are the important class of particles elongated in one direction with a constant cross-section of arbitrary shape. The cross-section A (with maximum dimension d) should be small in comparison to the length of the whole particle, L:

$$d \ll L; \quad L = \left(D^2 - d^2 \right)^{\frac{1}{2}} \approx D \tag{41}$$

The scattering curve of such a particle can be written as

$$I(h) = L\left(\frac{\pi}{h} \right) I_c(h) \tag{42}$$

where the function $I_c(h)$ is known as a cross-section function, and it is

$$I_c(h) = (L\pi)^{-1} I(h)h = \text{const } I(h)h = 2\pi \int_0^\infty p_c(r) J_0(hr) dr \tag{43}$$

where $J_0(hr)$ is the zero-order Bessel function [344], and the expression for the cross-section pair distance distribution function, $p_c(r)$ is

$$p_c(r) = \frac{1}{2\pi} \int_0^\infty I_c(h)(hr) J_0(hr) dh. \tag{44}$$

5.2.5.1.3. Flat particles. Flat particles, i.e., particles elongated in two dimensions (like a discs, flat prisms, etc.) with a constant thickness T, much smaller than the overall dimensions, D, can be treated in a similar way. The scattering function can be written as

$$I(h) = A \frac{2\pi}{h^2} I_t(h) \tag{45}$$

where $I_t(h)$ is the so-called thickness factor, A is the area of the flat particles [345]. The thickness scattering intensity function is

$$I_t(h) = (A2\pi)^{-1} I(h)h^2 = \text{const } I(h)h^2 \tag{46}$$

which can be used for the determination of R_t and T.

$$I_t(h) = 2 \int_0^\infty p_t(r) \cos(hr) dr. \tag{47}$$

$P(r)$ does not show clear features, and therefore, it is better to use $f(r) = p(r)/r$ [341].

5.2.5.2. Hollow and inhomogeneous particles.
If there is an internal inhomogeneity within the particles, it is impossible to get a unique reconstruction of an inhomogeneous three-dimensional structure from its scattering function without additional a priori information. Besides, $p(r)$ function can be negative. Therefore, the minimum in the $p(r)$ function can be caused by a small number of distances or by the addition of positive and negative contributions.

5.2.5.2.1. Spherically symmetric particles. It is possible to describe the particle by an one-dimensional radial excess density function, $\Delta\rho(r)$. The scattering amplitude is the Fourier transform of the radial distribution [342]:

$$A(h) = 4\pi \int_0^\infty r\rho(r) \frac{\sin(hr)}{(hr)} dr, \tag{48}$$

and

$$\rho(r) = \frac{1}{2\pi^2} \int_0^\infty hA(h) \frac{\sin(hr)}{r} dh. \tag{49}$$

$P(r)$ can be calculated from $I(h)$ using Eq. (37) remembering that this function is the convolution square of $\rho(r)$. Using a convolution square root technique $\rho(r)$ can be calculated from $I(h)$ via $p(r)$ avoiding a phase problem which is present in

crystallography, i.e., it is not necessary to calculate scattering amplitudes and phases [338]. This can be done because of the fact that $p(r)$ differs from zero only within the limited range $0 < r < D$. The scattering function and the $p(r)$ of a hollow sphere can be calculated. The $p(r)$ of the hollow sphere has a triangular shape, and the function $f(r) = p(r)/r$ shows a horizontal plateau [346].

5.2.5.2.2. Rod-like particles with radial inhomogeneity. If ρ is the function of the radius r, but not of the angle, some structural information can be calculated. If the average excess electron density in the cross-section is denoted as $\bar{\rho}_c$, and $p(r)$ exhibits a linear part within the region $r > d$, then $\Delta\rho$ can be replaced the by $\bar{\rho}_c$ with the maximum dimension of the cross-section d. The $p(r)$ function differs from that of a homogeneous cylinder with the same $\bar{\rho}_c$ only within the range $0 < r \leq d$.

5.2.5.2.3. Flat particles with cross-sectional inhomogeneity. Lamellar particles with varying electron density perpendicular to the basal plane show differences in the $p(r)$ within the range $0 < r < T$, compared to the homogeneous lamella of the same size, where T is the thickness of the lamella, and ρ is a function of the distance x from the central plane.

5.2.6. Polydisperse systems

The scattering function of a polydispersed system is determined by the particle shapes and by their size distribution [324,328,345,346]. A certain particle size distribution can be assumed, and after that the shape can be determined. A more frequent way is to assume the shape, and then the particle size distribution can be determined. It is supposed that there is scattering intensity from an ensemble of particles of the same shape, whose number size distribution can be described by a function $D_n(R)$, where R is the particle radius. It is also assumed that there are no interparticle interferences or multiple scattering effects. Then the scattering function $I(h)$ is given by

$$I(h) = c_n \int_0^\infty D_n(R) R^6 i_0(hr) \mathrm{d}R, \tag{50}$$

where c_n is a constant, the factor R^6 takes into account that the particle volume is proportional to R^3, and $i_0(hr)$ is the normalized form factor of a particle of size R [347]. In many cases, one may be interested in the volume distribution, $D_V(R)$ (sometimes called mass distribution $D_m(R)$), or in the intensity distribution, $D_i(R)$. In the case of a mass distribution, it stands

$$I(h) = c_m \int_0^\infty D_m(R) R^3 i_0(hr) \mathrm{d}R. \tag{51}$$

In investigations of the systems containing a small number of big particles and a large number of small particles, knowledge of the intensity distribution is very important. Although multiple scattering is not present in the experiment at low concentrations, effects of the interparticle interferences start to influence SAXS data much earlier, i.e., at lower concentration, than multiple scattering occurs. Multiple scattering becomes more dominant in the systems with increasing the

size, and with increasing the difference of the electronic density between the scatterers and the solvent (contrast). To eliminate these effects, a series of concentrations have to be measured, and then the extrapolation to zero concentration, c_0, can be done.

5.2.7. Data evaluation and interpretation

In this section, a very short description of data treatment and interpretation which has been explained in detail in the book "Small Angle X-ray Scattering" edited by O. Glatter and O. Kratky [344,346] will be given.

All theoretical equations in the previous sections correspond to the ideal conditions of instrumental equipment. In the real experiments, there is no measurement with a point-like parallel and strictly monochromatic primary beam, and the detector will have non-negligible dimensions. The finite size of the beam, its divergence, the detector size, and the wavelength distribution lead to an instrumental broadening. By these effects, the measured scattering curve is said to be smeared. In the scattering process, $p(r)$ function, not measured directly, is Fourier-transformed into the scattering function $I(h)$, that is smeared by the broadening effects. The final smeared scattering function, $I_{exp}(h)$, is measured with a certain experimental error, $\sigma(h)$. In the case of polydisperse systems, the situation is very similar. Size distribution function, $D(R)$, is a starting point and there is a different transformation, but the smearing problem is the same.

In order to get reliable results, it is necessary to perform a series of experiments, i.e., repeated experiments for every sample, for ensuring to estimate a mean value and a standard deviation at every scattering angle. This experimentally determined standard deviation is much higher than the standard deviation estimated from counting statistics. The experiment with a cuvette filled only with solvent is necessary for subtracting background scattering coming from the instruments and from the solvent. Finally, it is necessary to perform a series of such experiments at different concentrations for the extrapolation to zero concentration, i.e., the elimination of interparticle interferences. Therefore, it is necessary to have the so-called primary data handling routine that performs all preliminary steps (averaging, subtraction, normalization, overlapping, concentration extrapolation). In addition, it is very helpful to have the possibility of calculating the Guinier radius, the Porod extrapolation from the raw data. When all these steps have been performed, the final result is a smeared particle-scattering function, $I_{exp}(h)$, with a certain statistical reliability. $I(h)$, $p(r)$, and all particle parameters will be computed from these data sets. In order to do this, the function $I_{exp}(h)$ will be smooth and desmeared. The smoothing operation is an absolute necessity because the desmearing process is comparable to a differentiation which is impossible for noisy data. Finally, it is necessary to perform a Fourier transform to invert Eqs. (35) or (50) and (51).

Instrumental broadening can be separated into three components, the two-dimensional geometrical effects (slit-length and slit-width effects) and the wavelength effect. Each

effect can be described separately by an integral equation [344] and this threefold integral equation cannot be solved analytically:

$$\bar{I}_{\exp}(h) = 2 \int_{-\infty}^{\infty} \int_{0}^{\infty} \int_{0}^{\infty} Q(x)P(t)W(\lambda')I$$
$$\times \left(\frac{[(m-x)^2 + t^2]^{1/2}}{\lambda'} \right) d\lambda' \, dt \, dx. \tag{52}$$

Numerical methods have to be used for its solution. The indirect transformation method solves the problems of smoothing, desmearing and Fourier transformation in one step. Very short description of this technique will be given in the following section.

5.2.8. Principles of indirect Fourier transformation (IFT)

IFT requires the following operations: single-step procedure, optimised general function system, weighted least-squares approximation, transformation to real space with minimised termination effect, error propagation, and consideration of the physical smoothing condition given by the maximum interparticle distance [323,327,344,346]. The smoothing condition requires estimation of the maximal particle size, $D_{\max}$, and the upper limit for the largest particle dimension:

$$D_{\max} \geq D \tag{53}$$

$D_{\max}$ need not be estimated very precisely, but it must not be smaller than D. The procedure starts within the real space. Since the $p(r)$ function is equal to zero for all the values $r \geq D_{\max}$, $p(r)$ is used to represent the system and it is defined only within the space $0 \leq r \geq D_{\max}$. Without going into the details, the linear combination is used as an approximation of $p(r)$. A linear combination

$$p_A(r) = \sum_{v=1}^{N} c_v \varphi_v(r) \tag{54}$$

is used as an approximation to $p(r)$; N is the number of functions, and c are the unknowns. Functions $\varphi_v(r)$ are chosen as cubic B-splines. It is precisely known how to calculate a smeared scattering function, $\bar{I}(h)$ from $I(h)$, and how $p(r)$ or $D(r)$ is transformed into $I(h)$, but the inverse transformations are not known. All these transformations are linear and they can be applied to all terms in the sum. Hence, the approximation $I_A(h)$ to the ideal (unsmeared) scattering function can be written as

$$I_A(h) = \sum_{v=1}^{N} c_v \psi_v(h), \tag{55}$$

where the functions $\psi_v(h)$ are calculated from $\varphi_v(r)$, the coefficients c remain unknown. The final fit in the smeared space is given by the series

$$\bar{I}_A(h) = \sum_{v=1}^{N} c_v \chi_v(h) \tag{56}$$

where the $\chi_v(h)$ are functions calculated from $\psi_v(h)$. All three equations are similar because of the linearity of the transforms. The expression can be minimized

$$L = \sum_{k=1}^{M} \frac{(\bar{I}_{\exp}(h_k) - \bar{I}_A(h_k))^2}{\sigma^2(h_k)} \tag{57}$$

where M is the number of experimental points. To find the best solution, additional regularization techniques are necessary [342].

5.2.9. Determination of the system electron density; deconvolution of p(r) function

The electron density distribution, $\rho(r)$, as a three-dimensional structure, cannot be determined directly from a one-dimensional scattering function, i.e., from $I(h)$ or $p(r)$. Every direct method requires additional a priori information or assumptions about the investigated system. If that information describes the one-dimensional structure, there are good reasons to believe that the structure can be recognised from the scattering data. Typical examples are either particles with spherical symmetry where the electron density, ρ, depends only on the distance of the sphere centre, r, or particles with rod and lamellar symmetry where the electron density depends on the distance of the rod axis and on the distance from the central plane in the lamellae, respectively.

5.2.10. Application to surfactant systems; lamellar bilayers

If the unilamellar system is assumed with negligible in-plane scattering, i.e., Δ_t is only the function of the distance, r, from the central plane of the lamellae, monodispersed vesicles show high-frequency oscillations that correspond to the radius of the vesicle. Consequently, an ideal flat lamella shows zeros in the $I(h)$ function, but real systems show more or less pronounced minima (see Fig. 9). Inhomogeneity of particles causes the minimum in the range of $0 < r < 2R$, which can be positive or negative. The maximum was found by Iampietro et al. [99] and Maurer et al. [79].

Studies of the dynamics of morphological transitions in amphiphilic systems have become an increasingly active field in
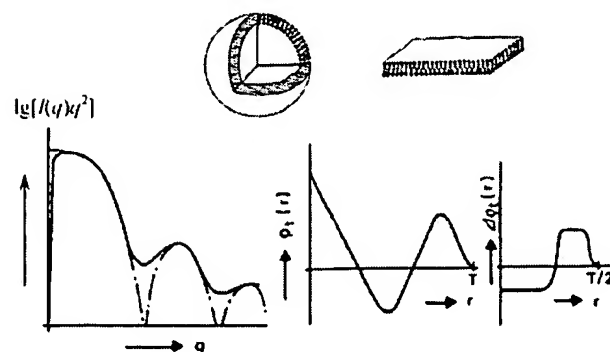

Fig. 9. Thickness functions, $I(q)q^2$, $p_t(r)$, and $\rho\Delta t(r)$ for vesicles and lamellae with thickness T. Reproduced from H. Brumberger, "Modern Aspects of Small Angle Scattering", Kluwer Academic Publishers, London, 1995, p. 137. With kind permission of Prof. Otto Glatter. With kind permission of Springer Science and Business Media.

colloid science. Recent advances in the time resolution of scattering experiments allow observation of structural changes down to a millisecond range. The experimental data could be explained quantitatively by a theoretical model. A detailed model for the formation of vesicles is given by Robinson et al. [202], based on the analysis in terms of the bending energy that allows the quantitative predictions. The fusion of membranes is currently a hot topic in colloidal science, with the highlight on its biological importance. Accordingly, a number of papers can be found where the dynamics of vesicle formation has been studied in detail, as well as descriptions of vesicle formation in the catanionic mixtures [50,99–101,205,228,237].

Formation of oblate micelles, vesicles, and very flexible bilayers in the region of the phase diagram between the micellar and lamellar phases of the binary double-tailed ionic surfactant sodium 4-(1-pentylheptyl) benzenesulphonate/water system was observed [348].

A detailed study of the important initial stages in the formation process of mesoporous materials in highly time-resolved scattering experiments, combining SAXS and SANS data was reported [349].

5.2.11. Small angle neutron scattering

SANS cannot compete in the quality of resolution with other techniques, like X-ray crystallography or multi-dimensional NMR, but it is a very useful tool for studying the native structures of biological macromolecules and of complexes in solution. Use of neutrons has an advantage over X-rays because the scattering power of neutrons varies strongly for the different kinds of biologically relevant matter, i.e., proteins, nucleic acids, lipids, and sugars. Since the physical principles of scattering are the same for all the scattering methods and for wide-angle diffraction, it is not necessary to go into the details of concepts and expressions as it is done in the case of SAXS. The interaction of neutrons with matter is different. Instead of electron density in SAXS, SANS has to deal with the so-called scattering length density. The essential fact in neutron scattering is the pronounced difference in the scattering length between hydrogen and deuterium, which is important for the variation of the contrast between the particles and the matrix. Another important feature of neutron scattering is the high incoherent scattering cross-section of hydrogen.

The phase behavior of mixtures of oppositely charged surfactants CTAB and SOS has been studied with [100] and without [101] added salt. In the absence of added salt, a large vesicle region exists in the SOS-rich side of the phase diagram. The addition of NaBr to a mixture of CTAB and SOA leads to destabilization of the vesicle phase and to the formation of the micellar phase. Calculations using the cell model were verified by contrast variation SANS [228]. The low q data were analyzed in the Guinier approximation to extract structural information about the aggregate. The development of the model-independent methodology [330,350] for the analysis of small-angle scattering data provides the more detailed information about the scattering particle. That methodology using indirect Fourier transformation followed by the deconvolution technique has been described [328,351] and outlined [351,352].

A SANS study of vesicles and lamellar sheets formed in the mixtures of SDS and DTAB was performed. Unilamellar or oligolamellar vesicles form in the most diluted samples. Transition from vesicles to stacks of lamellar sheets upon increasing the overall surfactant concentration was observed [353].

Similar investigations were performed on the association of amphiphilic polymers consisting of two tails attached onto poly (ethylene glycol) polymer chains in two different systems of equilibrium vesicles. For the system CTAB/sodium perfluorohexanoate, the size distribution of the vesicles slightly narrows in the presence of the polymer. In contrast, the confinement of polymer molecules inside the CTAB/sodium perfluorohexanoate vesicles was different. By comparison of the SANS results, e.g., the vesicle radius and the size distribution before and after adding the polymer, the polymer incorporation mechanism was understood [354].

A recent study of the spontaneous formation of vesicles in aqueous mixtures of polymerisable surfactants showed that stable vesicle structure can be fixed by polymerisation. Both native and polymerised vesicles are characterised using DLS, SLS, SANS and Cryo-TEM [203].

Bergström et al. performed the SANS investigation on the aggregates formed from aqueous mixtures of SDS and DTAB in the presence and absence of salt. Small unilamellar vesicles ($r=35–65$ nm) were found in highly diluted solutions, whereas larger oligolamellar vesicles predominated in dilute solutions of an almost equimolar surfactant composition. With the increase in surfactant concentration, transitions either from small unilamellar vesicles to micellar aggregates or from larger oligolamellar vesicles to lamellar sheets were observed [271].

6. Catanionic mixture

One of the most investigated ternary catanionic systems is DDAB/SDS/H_2O [83,84,86,89–91,93,238,280] which was first described by Kaler [50]. His approach using commercial single- and double-tailed surfactants resulted in a common method for the preparation of spontaneously formed vesicles of controlled sizes, surface charge, and permeability [355–357]. This method requires neither mechanical nor chemical perturbation. Simple mixing of the anionic and cationic components suffices for spontaneous formation of vesicles. The phase diagram of the ternary system (anion/cation/water) as well as the glucose trapping of vesicles was studied using microscopic techniques [83,84,205,237].

The DDAB/SDS/H_2O system is the most investigated ternary catanionic system [83,84,86,89–91,93,238,280]. Anionic surfactant SDS reacts with the cationic one due to the strong electrostatic interaction, and therefore, a catanionic salt is formed. Also, a number of new phases and structures were determined. Each phase in such a mixed system was formed according to the packing parameter as well as to the concentration of each surfactant. The phase diagram of the mixture DDAB/SDS/H_2O at 40 °C shows an isotropic solution, lamellar phase, cubic phase, and crystal phase [89].

Addition of an anionic surfactant to the lamellar phase in the system DDAB/H$_2$O causes several effects. Electrostatic interactions between the surfactant heads result in a decrease of spontaneous curvature of aggregates, increasing their size, or forming a new structure. Influences on the size and stability of catanionic vesicles were investigated by different preparation methods, i.e., by sonication, and by aging [238].

Precipitation of the catanionic salt equilibrated with the lamellar phase occurs close to the equimolar ratio [84]; the solubility of the salt is very low. The DDAB vesicular bilayer is capable of incorporating a certain amount of anionic surfactant without interrupting the former structure. The amount of 1 wt.% DDAB allows almost 25 mol% of SDS to be incorporated into the vesicular bilayer without destroying the structure. Anionic surfactant SDS is responsible for the thermodynamic stabilisation of vesicles as well as for the change of vesicle sizes [86]. In the whole area of DDAB excess, the formation of mixed micelles as well as of mixed vesicles was observed. The region of unilamellar vesicles having radii under 100 nm was found. The macroscopic phase with small globular or discotic micelles in eqilibrium with vesicles was also observed. In that area, SDS addition caused changes in vesicle sizes, showing complex competition between the geometric packing and the electrostatic interaction [86]. In the DDAB/SDS/H$_2$O system, the presence of large unilamellar micrometer vesicles (0.1–5 μm) with high polydispersity was detected by pulsed field gradient NMR self-diffusion [84,86].

Kondo et al. investigated the encapsulation of glucose into the SDS/DDAB vesicles; large poydisperse vesicles ($d \sim 40$ μm) were observed using DIC LM [83].

Bergström et al. investigated the aggregate structures in the above-described mixtures using SANS [280]. The mixture contains micelles of three-axes ellipsoid shape (semi-axes: $a = 14$ Å, $b = 23$ Å, $c = 27$ Å) at 1 wt.% of total surfactant, and at mole fraction SDS, $X = 0.95$. By dilution the sample to a total surfactant percentage less than 1 wt.%, small unilamellar vesicles were formed, since under 0.2 wt.% of total surfactant, the middle radius of vesicles increased.

A diluted solution of catanionic SDS/DDAB vesicles was also investigated by DSC. In that experiment, the temperature of the gel–liquid phase transition was found for the mixed vesicles. Addition of the salt decreases the transition temperature. The phenomenon was explained by electrostatic interactions, which influenced the packing of chains and the temperature of the phase transition [90]. The enthalpies of the formation of: catanionic crystals (-125.8 kJ mol^{-1}), vesicles (41.23 kJ mol^{-1}), and the vesicle–micelle transition (32.10 kJ mol^{-1}) were determined [91]. In the mixed system, cmc is lowered compared to cmc of each surfactant. Addition of a double-tailed surfactant into the mixture causes a synergetic effect due to its strong hydrophobic character.

7. Concluding remarks

Both the fascination with the self-organisation, shapes, sizes, inner structures of vesicles and the huge importance of vesicles, particularly in life sciences, are the driving forces for such tremendous interest in vesicle research. Although this review has attempted to gather the latest investigations on the spontaneous formation of vesicles (which is a small part of the comprehensive vesicle research), very soon, someone will find newer publications. The molecules forming vesicles, methods of vesicles preparation, and techniques for their structure and properties determination, as well as many relevant examples, are included in the review.

Acknowledgement

References

[1] Tanford Ch. Monolayers, micelles, lipid vesicles and biomembranes. In: Degiorgio V, Corti M, editors. Physics of amphiphiles: micelles, vesicles and microemulsions. Bologna: Elsevier Science; 1985. p. 547–54.

[2] Woodle MC. Adv Drug Deliv Rev 1995;16:249–65.

[3] Hagstrom JE, Sebestyen MG, Budker V, Ludtke JJ, Fritz JD, Wolff JA. Biochim Biophys Acta 1996;1284:47–55.

[4] Lasic DD, Papahadjopoulos D. Curr Opin Solid State Mater Sci 1996;1:392–400.

[5] Tseng WC, Haselton FR, Giorgio TD. Biochim Biophys Acta 1999;1445:53–64.

[6] Moenkkoenen J, Urtti A. Adv Drug Deliv Rev 1998;34:37–49.

[7] Zabner J. Adv Drug Deliv Rev 1997;27:17–28.

[8] Lasic DD. Trends Biotechnol 1998;16:307–21.

[9] Lasic DD. J Control Release 1997;48:203–22.

[10] Gradzielski M. Curr Opin Colloid Interface Sci 2004;9:149–53.

[11] Gradzielski M. Curr Opin Colloid Interface Sci 2003;8:337–45.

[12] Svenson S. Curr Opin Colloid Interface Sci 2004;9:201–12.

[13] Schurtenberger P, Bertani R, Kaenzig W. J Colloid Interface Sci 1986;114:82–7.

[14] Bangham AD, Horne RW. J Mol Biol 1964;8:660–8.

[15] Lasic DD. Giant vesicles: a historical introduction. In: Luisi Pier Luigi, Walde Peter, editors. Giant vesicles, perspectives in supramolecular chemistry, vol. 6. Chichester: John Wiley & Sons, Ltd.; 2000.

[16] Gobley M. J Pharm Chim 1847;17:401.

[17] Lehmann O. Z Phys Chem 1889;4:462–72.

[18] Neubaurer C. Z Anal Chem 1867;6:189.

[19] Gordel E, Grendel F. J Exp Med 1925;41:439.

[20] Sheppard SE, Lambert RH. J Franklin Inst 1929;207:137.

[21] Sheppard SE, Lambert RH. J Franklin Inst 1927;203:158–9.

[22] Wilsey RB. J Franklin Inst 1925;200:739–46.

[23] Bangham AD, Standish MM, Watkins JC. J Mol Biol 1965;13:238–52.

[24] Saunders L, Perrin J, Gammack D. J Pharm Pharmacol 1962;14:567–72.

[25] Robinson N. J Pharm Pharmacol 1960;12:129–49.

[26] Robinson N. J Pharm Pharmacol 1960;12:193–218.

[27] Wick R, Angelova MI, Walde P, Luisi PL. Chem Biol 1996;3:105–11.

[28] Watwe RM, Bellare JR. Curr Sci 1995;68:715–24.

[29] Hauser H. Proc Natl Acad Sci 1989;86:5351–5.

[30] Papahadjopoulos D, Watkins JC. Biochim Biophys Acta 1967;135:639–52.

[31] Johnson SM, Bangham AD, Hill MW, Korn ED. Biochim Biophys Acta 1971;233:820–6.

[32] Huang CH. Biochemistry 1969;8:344–52.

[33] Wang W, Tetley L, Uchegbu IF. J Colloid Interface Sci 2001;237:200–7.

[34] Gebicki JM, Hicks M. Chem Phys Lipids 1976;16:142–60.

[35] Hicks M, Gebicki JM. Chem Phys Lipids 1977;20:243–52.

[36] Cohen BE. Biochim Biophys Acta 1986;857:117–22.

[37] Grant CWM, Hamilton KS, Hamilton KD, Barber KR. Biochim Biophys Acta 1989;984:11–20.

[38] Powderly WG, Kobayashi GS, Herzig GP, Medoff G. Am J Med 1988;84:826–32.

[39] Robertson MJ, Larson RA. Am J Med 1988;84:233–9.

[40] Karp JE, Burch PA, Merz WG. Am J Med 1988;85:203–6.

[41] Sculier JP, Coune A, Meunier F, Brassinne C, Laduron C, Hollaert C, et al. Eur J Cancer Clin Oncol 1988;24:527–38.

[42] Coune A. Eur J Cancer Clin Oncol 1988;24:117–21.

[43] Presant CA, Multhauf P, Metter G. Eur J Cancer Clin Oncol 1987;23:683–7.

[44] Washington C, Taylor SJ, Davis SS. Int J Pharm 1988;46:25–30.

[45] Weber G, Jayaram HN, Pillwein K, Natsumeda Y, Reardon MA, Zhen YS. Adv Enzym Regul 1987;26:335–52.

[46] Reynolds JA. Surfactants and lipid vesicles as tools in biological research. In: Degiorgio V, Corti M, editors. Physics of amphiphiles: micelles, vesicles and microemulsions. Elsevier Science; 1985. p. 555–62.

[47] Kaler EW, Falls AH, Davis HT, Scriven LE, Miller WG. J Colloid Interface Sci 1982;90:424–43.

[48] Hamilton RT, Kaler EW. J Colloid Interface Sci 1987;116:248–55.

[49] Martino A, Kaler EW. Colloids Surf A 1995;99:91–9.

[50] Kaler EW, Murthy AK, Rodriquez BE, Zasadzinski JAN. Science 1989;245:1371–4.

[51] Morgan JD, Johnson CA, Kaler EW. Langmuir 1997;13:6447–51.

[52] Fendler H. Chem Rev 1987;87:877–99.

[53] Hammond K, Lyle IG, Jones MN. Colloids Surf A 1987;23:241–57.

[54] Seifert U, Berndl K, Lipowsky R. Phys Rev A 1991;44:1182–202.

[55] Svard M, Schurtenberger P, Fontell K, Joensson B, Lindman B. J Phys Chem 1988;92:2261–70.

[56] Kunieda H, Nakamura K, Olsson U, Lindman B. J Phys Chem 1993;97:9525–31.

[57] Laughlin RG. Colloids Surf A 1997;128:27–38.

[58] Bhandarkar S, Bose A. J Colloid Interface Sci 1990;135:531–8.

[59] Kölchens S, Ramaswami V, Birgenheier J, Nett L, O'Brien DF. Chem Phys Lipids 1993;64:1–10.

[60] Marques EF. Langmuir 2000;16:4798–802.

[61] Hauser H, Gains N, Müller M. Biochemistry 1983;22:4775–81.

[62] Evans E, Needham D. Faraday Discuss Chem Soc 1986;81:267–81.

[63] Mann S, Hannington JP, Williams RJP. Nature 1986;324:565–7.

[64] Rydhag L, Stenius P, Oedberg L. J Colloid Interface Sci 1982;86:274–6.

[65] Regev O, Guillemet F. Langmuir 1999;15:4357–64.

[66] Morigaki K, Walde P, Misran M, Robinson BH. Colloids Surf A 2003;213:37–44.

[67] Olsonh F, Hunt CA, Szoka FC, Vail WJ, Papahadjopoulos D. Biochim Biophys Acta 1979;557:9–23.

[68] Mayer LD, Hope MJ, Cules PR. Biochim Biophys Acta 1986;858:161–8.

[69] Edwaards K, Almgren M, Bellare J, Brown W. Langmuir 1989;5:473–8.

[70] Imura T, Yanagishita H, Ohira J, Sakai H, Abe M, Kitamoto D. Colloids Surf B Biointerfaces 2005;43:115–21.

[71] Baba T, Minamikawa H, Hato M, Motoki A, Hirano M, Zhou D, et al. Biochem Biophys Res Commun 1999;265:734–8.

[72] Polidoria A, Puccia B, Zarif L, Lacombea J-M, Riess JG, Pavia AA. Chem Phys Lipids 1995;77:225–51.

[73] Zheng L-Q, Shui L-I, Shen Q, Li G-Z, Baba T, Minamikawa H, Hato M. Colloids Surf A 2002;207:215–21.

[74] Sundler R. Biochim Biophys Acta—Biomembr 1984;771:59–67.

[75] Lasic DD. Liposomes: from physics to applications. Amsterdam: Elsevier; 1993.

[76] Lockhoff O. Angew Chem Int Ed Engl 1991;30:1611.

[77] Baba T, Zheng L-Q, Minamikawa H, Hato M. J Colloid Interface Sci 2000;223:235–43.

[78] Zhu J, Yan F, Guo Z, Marchant RE. J Colloid Interface Sci 2005;289:542–50.

[79] Maurer N, Glatter O, Hofer M. J Appl Chryst 1991;24:832–5.

[80] Kitamoto D, Isoda H, Nakahara T. J Biosci Bioeng 2002;94:187–201.

[81] Lang S. Curr Opin Colloid Interface Sci 2002;7:12–20.

[82] Karukstis KK, Zielaniuk CA, Fox MJ. Langmuir 2003;19:10054–60.

[83] Kondo Y, Uchiyama H, Yoshino N, Nishiyama K, Abe M. Langmuir 1995;11:2380–4.

[84] Marques EF, Regev O, Khan A, da Graca Miquel M, Lindman B. J Phys Chem B 1998;102:6746–58.

[85] Talmon Y, Evans DF, Ninham BW. Science 1983;221:1047–8.

[86] Marques EF, Regev O, Khan A, da Graca Miquel M, Lindman B. J Phys Chem B 1999;103:8353–63.

[87] Filipović-Vinceković N, Bujan M, Šmit I, Tušek-Božić Lj, Štefanić I. J Colloid Interface Sci 1998;201:59–70.

[88] Karukstis KK, Suljak SW, Waller PJ, Whiles JA, Thompson EHZ. J Phys Chem 1996;100:11125–32.

[89] Marques E, Khan A, de Graca Miquel M, Lindman B. J Phys Chem 1993;97:4729–36.

[90] Marques EF, Khan A, Lindman B. Thermochim Acta 2002;394:31–7.

[91] Bai G, Wang Y, Wang J, Han B, Yan H. Langmuir 2001;17:3522–5.

[92] Das Burman A, Dey T, Mukherjee B, Das AR. Langmuir 2000;16:10020–7.

[93] Bumajdad A, Eastoe J, Griffiths P, Steytler DC, Heenan RK, Lu JR, et al. Langmuir 1999;15:5271–8.

[94] Murthy K, Easwar N, Singer E. Colloid Polym Sci 1998;276:940–4.

[95] Chen WJ, Zhai LM, Li GZ, Li BQ, Xu J. J Colloid Interface Sci 2004;278:447–52.

[96] Vautrin C, Zemb T, Schneider M, Tanaka M. J Phys Chem B 2004;108:7986–91.

[97] Yan Y, Xiong W, Huang J, Li Z, Li X, Li N, et al. J Phys Chem B 2005;109:357–64.

[98] de Graca Miquel M, Pais AACC, Dias RS, Leal C, Rosa M, Lindman B. Colloids Surf A 2003;228:43–55.

[99] Iampietro DJ, Brasher LL, Kaler EW, Stradner A, Glatter O. J Phys Chem B 1998;102:3105–13.

[100] Brasher LL, Herrington KL, Kaler EW. Langmuir 1995;11:4267–77.

[101] Yatcilla MT, Herrington KL, Brasher LL, Kaler EW, Chiruvolu S, Zasadzinski JA. J Phys Chem 1996;100:5874–9.

[102] Vinceković M, Bujan M, Šmit I, Filipović-Vinceković N. Colloids Surf A 2005;255:181–91.

[103] Antunes FE, Marques EF, Gomes R, Thuresson K, Lindman B, Miguel MG. Langmuir 2004;20:4647–56.

[104] Grillo I, Kats EI, Muratov AR. Langmuir 2003;19:4573–81.

[105] Gonzáles YI, Stjerndahl M, Danino D, Kaler EW. Langmuir 2004;20:7053–63.

[106] Šegota S, Heimer S, Težak Đ. Colloids Surf A 2006;274:91–3;
Šegota S, Heimer S, Težak Đ. Colloids Surf A 2006;280:245;
Šegota S. Fractal clusters of association colloids, Ph.D. Thesis, Zagreb, 2003.

[107] Hao J, Hoffmann H. Curr Opin Colloid Interface Sci 2004;9:279–93.

[108] Oda R, Bourdieu L, Schmutz M. J Phys Chem B 1997;101:5913–6.

[109] Oberdisse J, Regev O, Porte G. J Phys Chem B 1998;102:1102–8.

[110] Hoffmann H, Thunig C, Miller D. Colloids Surf A 2002;210:147–58.

[111] Goldraich M, Schwartz JR, Burns JL, Talmon Y. Colloids Surf A 1997;125:231–44.

[112] Danino D, Weihs D, Zana R, Oraedd G, Lindblom G, Abe M, Talmon Y. J Colloid Interface Sci 2003;259:382–90.

[113] Lemp E, Zanocco AL, Guenther G. Colloids Surf A 2003;229:63–73.

[114] Gradzielski M, Bergmeier M, Hoffmann H, Mueller M, Grillo I. J Phys Chem B 2000;104:11594–7.

[115] Kabanov AV, Bronich TK, Kabanov VA, Yu K, Eisenberg A. J Am Chem Soc 1998;120:9941–2.

[116] Roversi M, La Mesa C. J Colloid Interface Sci 2005;284:470–6.

[117] Robertson D, Hellweg T, Tiersch B, Koetz J. J Colloid Interface Sci 2004;270:187–94.

[118] Ma G, Cheng Q. Langmuir 2005;21:6123–6.

[119] Limin Z, Ganzuo L, Zhiwei S. Colloids Surf A 2001;190:275–83.

[120] Zhai L, Zhang J, Shi Q, Chen W, Zhao M. J Colloid Interface Sci 2005;284:698–703.

[121] Cha JN, Birkrdal H, Euliss LE, Bartl MH, Wong MS, Deming TJ, et al. J Am Chem Soc 2003;125:8285–9.

[122] Moreau L, Grinstaff MW, Barthelemy P. Tetrahedron Lett 2005;46:1593–6.

[123] Simberg D, Weisman S, Talmon Y, Barenholz Y. Crit Rev Ther Drug Carr Syst 2004;21:257–317.

[124] Afri M, Ehrenberg B, Talmon Y, Schmidt J, Cohen Y, Frimer AA. Chem Phys Lipids 2004;131:107–21.

[125] Weisman S, Hirsch-Lerner D, Barenholz Y, Talmon Y. Biophys J 2004;87:609–14.

[126] Liang Z, Wang C, Huang J. Colloids Surf A 2003;224:213–20.

[127] Johnsson M, Wagenaar A, Stuart MCA, Engberts JBFN. Langmuir 2003;19:4609–18.

[128] Wang X, Wang J, Wang Y, Ye J, Yan H, Thoams RK. J Phys Chem B 2003;107:11428–32.

[129] Danino D, Talmon Y, Zana R. Langmiur 1995;11:1448–56.

[130] Menger FM, Chen XY, Brocchini S, Hopkins HP, Hamilton D. J Am Chem Soc 1993;115:6600–8.

[131] Guilbot J, Benvegnu T, Legros N, Plusquellec D, Dedieu JC, Gulik A. Langmuir 2001;17:613–8.

[132] Liang KN, Hui YZ. J Am Chem Soc 1992;114:6588–90.

[133] Israelachvili JN, Mitchell DJ, Ninham BW. Biochim Biophys Acta 1977;470:185–201.

[134] Israelachvili JN, Mitchell DJ, Ninham BW. J Chem Soc Faraday Trans 1976;72:1525–68.

[135] Nagarajan R. Langmuir 2002;18:31–8.

[136] Edlund H, Sadaghiani A, Khan A. Langmuir 1997;13:4953–63.

[137] Mitchell J, Ninham BW. J Chem Soc Faraday Trans 1981;77:601–29.

[138] Israelachvili JN. Intermolecular and surface forces, second edition with applications to colloidal and biological systems. London: Academic Press; 1985.

[139] Holmberg K, Joensson B, Kronberg B, Lindman B. Surfactants and polymers in aqueous solution. New York: John Wiley & Sons; 2002.

[140] Hiemenz PC, Rajagopalan R. Principles of colloid and surfaces chemistry. New York: Marcel Dekker, Inc.; 1997.

[141] Tanford C. J Phys Chem 1972;76:3020–4.

[142] Ostrowsky N, Sornette D. Interactions between nonionic vesicles. importance of the aliphatic-chain phase transition. In: Degiorgio V, Corti M, editors. Physics of amphiphiles: micelles, vesicles and microemulsions. Bologna: Elsevier Science; 1985. p. 563–86.

[143] Ninham BW, Evans DF. Faraday Discuss Chem Soc 1986;81:1–17.

[144] Tartar HV, Lelong AL. J Phys Chem 1956;59:1185–90.

[145] Evans DF, Ninham BW. J Phys Chem 1986;90:226–34.

[146] Gradzielski M. J Phys Condens Matter 2003;15:656–97.

[147] Gradzielski M, Muller M, Bergmeier M, Hoffmann H, Hoinkis E. J Phys Chem 1999;103:1416–24.

[148] Workshop on "Giant Vesicles", Centro Stefano Franscini, Switzerland, June 21–25, 1998.

[149] Kralj-Iglic V, Gomiscek G, Majhenc J, Arrigler V, Svetina S. Colloids Surf A 2001;181:315–8.

[150] Bozic B, Svetina S. Eur Biophys J Biophys Lett 2004;33:565–71.

[151] Bozic B, Gomiscek G, Kralj-Iglic V, Svetina S, Zeks B. Eur Biophys J Biophys Lett 2002;31:487–96.

[152] van der Linden E, Buytenhek CJ. Physica A 1997;245:1–10.

[153] Panizza P, Colin A, Coulon C, Roux D. Eur Phys J 1998;4:65–74.

[154] Oliviero C, Coppola L, Gianferri R, Nicotera I, Olsson U. Colloids Surf A 2003;228:85–90.

[155] Menger FM, Lee SJ, Keiper JS. Langmuir 1996;12:4479–80.

[156] Huang JB, Zhu BY, Zhao GX, Zhang ZY. Langmuir 1997;13:5759–61.

[157] Salkar RA, Mukesh D, Samant SD, Manohar C. Langmuir 1998;14:3778–82.

[158] Feitosa E, Barreleiro PCA, Olofsson G. Chem Phys Lipids 2000;105:201–13.

[159] Szoka F, Papahadjopoulos D. Annu Rev Biophys Bioeng 1980;9: 467–508.

[160] Joannic R, Auvray L, Lasic DD. Phys Rev Lett 1997;78:3402–5.

[161] Angelova MI, Soleau S, Melerd Ph, Faucon JF, Bothorel P. Prog Colloid Polym Sci 1992;89:127–31.

[162] Gabriel NE, Roberts MF. Biochemistry 1984;23:4011–5.

[163] Peschka R, Purmann T, Schubert R. Int J Pharm 1998;162:177–83.

[164] Luisi PL. Why giant vesicles. In: Luisi Pier Luigi, Walde Peter, editors. Giant vesicles, perspectives in supramolecular chemistry, vol. 6. Chichester: John Wiley & Sons, Ltd.; 2000. p. 3.

[165] Maguire LA, Zhang H, Shamlou PA. Biotechnol Appl Biochem 2003;37:73–81.

[166] Hamilton Jr R, Goerke L, Guo L, Williams M, Havel R. J Lipid Res 1980;21:981–92.

[167] Pupo E, Padrón A, Santana E, Sotolongo J, Quintana D, Dueñas S, et al. J Control Release 2005;104:379–96.

[168] Farmer MC, Gaber BP. Biophys J 1984;45:201.

[169] Lasic DD, Kidrič J, Zagorc S. Biochim Biophys Acta 1987;896:117–22.

[170] Douliez JP, Lavenant L, Renard D. J Colloid Interface Sci 2003;266:477–80.

[171] Schurtenberger P, Svard M, Wehrli E, Lindman B. Biochim Biophys Acta 1986;882:465–8.

[172] Edwards DA, Schneck F, Zhang I, Davis AMJ, Chen H, Langer R. Biophys J 1996;71:1208–14.

[173] Lasic DD. J Colloid Interface Sci 1988;124:428–35.

[174] Pautot S, Frisken BJ, Weitz DA. Proc Natl Acad Sci 2003;100:10718–21.

[175] Devaux PF. Biochemistry 1991;30:1163–73.

[176] Berndl K, Kas J, Lipowsky R, Sackmann E, Seifert U. Europhys Lett 1990;13:659–64.

[177] Batzri S, Korn E. Biochim Biophys Acta 1973;298:1015–9.

[178] Kramer JMH, Esker MWJ, Pathmamanoharan C, Wiesena PH. Biochemistry 1977;17:3932–5.

[179] Carmona-Ribeiro AM, Chaimovich H. Biochim Biophys Acta 1983;733:172–9.

[180] Nascimento DB, Rapuano R, Lessa MM, Carmona-Ribeiro AM. Langmuir 1998;14:7387–91.

[181] Cuccovia IM, Feitosa E, Chaimovich H, Sepulveda L, Reed W. J Phys Chem 1990;94:3722–5.

[182] Cuccovia IM, Sesso A, Abuin EB, Okino PF, Tavares PG, Campos JFS, et al. J Mol Liq 1997;72:323–86.

[183] Kim S, Martin GM. Biochim Biophys Acta 1981;646:1–9.

[184] Kim S, Turker MS, Chi E, Sela S, Martin GM. Biochim Biophys Acta 1983;728:339–48.

[185] Buboltz JT, Feigenson GW. Biochim Biophys Acta 1999;1417:132–45.

[186] Zawada Z. Cell Mol Biol Lett 2004;9:589–602.

[187] Zawada Z. Cell Mol Biol Lett 2004;9:603–15.

[188] Bachmann D, Brandl D, Gregoriadis G. Int J Pharm 1993;91:69–74.

[189] Brandl M, Bachmann D, Drechsler M, Bauer KH. Drug Dev Ind Pharm 1990;16:2167–91.

[190] Sorgi FL, Huang L. Int J Pharm 1996;144:131–9.

[191] Talsma H, Ozer AY, Van Bloois L, Crommelin DJA. Drug Dev Ind Pharm 1989;15:197–207.

[192] Soon SY, Harbidge J, Titchener-Hooker NJ, Ayazi-Shamlou P. J Chem Eng Jpn 2001;10:10–1.

[193] Zhang L, Eisenberg A. Science 1995;268:1728–31.

[194] Zhang L, Bartels C, Yu Y, Shen H, Eisenberg A. Phys Rev Lett 1997;79:5034–7.

[195] Eisenberg A, Shen H. J Phys Chem B 1999;103:9473–87.

[196] Luo L, Eisenberg A. J Am Chem Soc 2001;123:1012–3.

[197] Jenekhe SA, Chen XL. Science 1998;279:1903–7.

[198] Yu K, Eisenberg A. Macromolecules 1996;29:6359–61.

[199] Luo L, Eisenberg A. Langmuir 2001;17:6804–11.

[200] Nardin C, Hirt T, Leukel J, Meier W. Langmuir 2000;16:1035–41.

[201] Majewski J, Wong JY, Park CK, Seitz M, Israelachvili JN, Smith GS. Biophys J 1998;75:2363–7.

[202] Bucak S, Robinson BH, Fontana A. Langmuir 2002;18:8288–94.

[203] Liu S, Gonzalez YI, Kaler EW. Langmuir 2003;19:10732–8.

[204] Kamenka N, Chorro M, Talmon Y, Zana R. Colloids Surf A 1992;67:213–22.

[205] Kaler EW, Herrington KL, Murthy AK, Zasadzinski JAN. J Phys Chem 1992;96:6698–707.

[206] Munkert U, Hoffmann H, Thunig C, Meyer HW, Richter W. Prog Colloid Polym Sci 1993;93:137–45.

[207] Schurtenberger P, Mazer N, Waldvogel S, Kanzig W. Biochim Biophys Acta 1984;775:111–4.

[208] Donath E, Sukhorukov B, Caruso F, Davis SA, Möhwald H. Angew Chem Int Ed 1998;37:2202–3.

[209] Carmona-Ribeiro AM. Chem Soc Rev 1992:209–14.

[210] Bernard AL, Guedeau-Boudeville MA, Artzner VM, Gulik-Krzywicki T, Meglio JM, Jullien L. J Colloid Interface Sci 2005;287:298–306.

[211] Nagawa Y, Regen SL. J Am Chem Soc 1991;113:7237–40.

[212] Nagawa Y, Regen SL. J Am Chem Soc 1992;114:1668–72.

[213] Naka K, Sadownik A, Regen SL. J Am Chem Soc 1992;114:4011–3.

[214] Liu Y, Regen SL. J Am Chem Soc 1993;115:708–13.

[215] Shibakami M, Inagaki M, Regen SL. J Am Chem Soc 1997;119:354–7.

[216] Blumenthal R, Clague MJ, Durell SR, Epand RM. Chem Rev 2003;103:53–70.

[217] Bradley JC, Guedeau-Boudeville M-A, Jeandeau G, Lehn J-M. Langmuir 1997;13:2457–62.

[218] Diat O, Roux D, Nallet F. J Phys II 1993;3:1427–52.

[219] Diat O, Roux D. J Phys II 1993;3:9–14.

[220] Frittz G, Wagner NJ, Kaler EW. Langmuir 2003;19:8709–14.

[221] Watanabe K, Nakama Y, Yanaki T, Hoffmann H. Langmuir 2001;17:7219–24.

[222] Mendes E, Narayanan J, Oda R, Kern F, Candau SJ, Monohar C. J Phys Chem B 1997;101:2256–8.

[223] Mendes E, Oda R, Monohar C, Narayanan J. J Phys Chem B 1998;102:338–43.

[224] Hao J, Hoffmann H, Horbaschek K. J Phys Chem B 2000;104:10144–53.

[225] Horbaschek K, Hoffmann H, Hao J. J Phys Chem B 2000;104:2781–4.

[226] Hao J, Hoffmann H, Horbaschek K. Langmuir 2001;17:4151–60.

[227] Tondre C, Caillet C. Adv Colloid Interface Sci 2001;93:115–34.

[228] Brasher LL, Kaler EW. Langmuir 1996;12:6270–6.

[229] Madani H, Kaler EW. Langmuir 1990;6:125–32.

[230] Iampietro DJ, Kaler EW. Langmuir 1999;15:8590–601.

[231] Raghavan SR, Fritz G, Kaler EW. Langmuir 2002;18:3797–803.

[232] Hentze HP, Raghavan SR, McKelvey CA, Kaler EW. Langmuir 2003;19:1069–74.

[233] González YI, Nakanishi H, Stjerndahl M, Kaler EW. J Phys Chem B 2005;109:11675–82.

[234] McKelvey CA, Kaler EW, Zasadzinski JA, Coldren B, Jung H-T. Langmuir 2000;16:8285–90.

[235] Söderman O, Herrington KL, Kaler EW, Miller DD. Langmuir 1997;13:5531–8.

[236] Chiruvolu S, Israelachvili JN, Naranjo E, Xu Z, Zasadzinski JA, Kaler EW, et al. Langmuir 1995;11:4256–66.

[237] Herrington KL, Kaler EW, Miller DD, Zasadinski JA, Chiruvolu S. J Phys Chem 1993;97:13792–802.

[238] Marques EF. Langmuir 2000;16:4798–802.

[239] Bergström M. Langmuir 1996;12:2454–63.

[240] Caillet C, Hebrant M, Tondre C. Langmuir 2000;16:9099–102.

[241] Safran SA, Pincus P, Andelman D. Science 1990;248:354–6.

[242] Hoffmann H, Thunig C, Schmiedel P, Munkert U. Langmuir 1994;10:3972–81.

[243] Marques EF, Regev O, Khan A, da Graca Miguel M, Lindman B. Macromolecules 1999;32:6626–37.

[244] Fontell K, Ceglie A, Lindman B, Ninham B. Acta Chem Scand A 1986;40:247–56.

[245] Khan A, Fontell K, Lindblom G, Lindman B. J Phys Chem 1982;86:4266–71.

[246] Lindman B, Ahlnäs T, Almgren M, Fontell K, Jönsson B, Khan A, et al. Finn Chem Lett 1982:74–85.

[247] Gradzielski M. J Phys Condens Matter 2003;15:656–97.

[248] Marques EF, Regev O, Khan A, Lindman B. Adv Colloid Interface Sci 2003;100–102:83–104.

[249] Tondre C, Caillet C. Adv Colloid Interface Sci 2001;93:115–34.

[250] Khan A, Marques EF. Curr Opin Colloid Interface Sci 2000;4:402–10.

[251] Lopez-Montero I, Rodriguez N, Cribier S, Pohl A, Velez L, Devaux PF. J Biol Chem 2005;280:25811–9.

[252] Taneva SG, Patty PJ, Frisken BJ, Cornell RB. Biochemistry 2005;44:9382–93.

[253] Tsogas I, Tsiourvas D, Nounesis G, Paleos CM. Langmuir 2005;21:5997–6001.

[254] Namani T, Walde P. Langmuir 2005;21:6210–9.

[255] Rossetti FF, Bally M, Michel R, Textor M, Reviakine I. Langmuir 2005;21:6443–50.

[256] Wang HY, Li YM, Xiao Y, Zhao YF. J Colloid Interface Sci 2005;287:307–11.

[257] Hargreaves WR, Deamer DW. Biochemistry 1978;17:3759–68.

[258] Ninham BW, Evans DF, Wei GJ. J Phys Chem 1983;87:5020–5.

[259] Brady JE, Evans DF, Kacher B, Ninham BW. J Am Chem Soc 1984;106:4279–80.

[260] Yeh SJ, Yang YM, Chang CH. Langmuir 2005;21:6179–84.

[261] Yu WY, Yang YM, Chang CH. Langmuir 2005;21:6185–93.

[262] Hoffmann H, Gräbner D, Hornfeck U, Platz G. J Phys Chem B 1999;103:611–4.

[263] Gebicki JM, Hicks M. Nature 1973;243:232–4.

[264] Chen WJ, Li GZ, Zhou GW, Zhai LM, Li ZM. Chem Phys Lett 2003;374:482–6.

[265] Cavallaro G, Giammona G, Manna GL, Palazzo S, Pitarresi G, Liveri VC. Int J Pharm 1993;90:195–201.

[266] Rodriguez MP, Prieto G, Rega C, Varela LM, Sarmiento F, Mosquera V. Langmuir 1998;14:4422–6.

[267] Tadros ThF. Surfactants. London: Academic Press; 1983.

[268] Yaacob II, Bose A. J Colloid Interface Sci 1996;178:638–47.

[269] Talhout R, Engberts JBFN. Langmuir 1997;13:5001–6.

[270] Meagher RJ, Hatton TA, Bose A. Langmuir 1998;14:4081–7.

[271] Bergström M, Pedersen JS. Langmuir 1998;14:3754–61.

[272] Bergström M, Pedersen JS. Langmuir 1999;15:2250–3.

[273] Bergström M, Pedersen JS. J Phys Chem B 1999;103:8502–13.

[274] Koehler RD, Raghavan SR, Kaler EW. J Phys Chem B 2000;104:11035–44.

[275] O'Connor AJ, Hatton TA, Bose A. Langmuir 1997;13:6931–40.

[276] Viseu MI, Edwards K, Campos CS, Costa SMB. Langmuir 2000;16:2105–14.

[277] Walker SA, Zasadzinski J. Langmuir 1997;13:5076–81.

[278] Fischer A, Hebrant M, Tondre C. J Colloid Interface Sci 2002;248:163–8.

[279] Herzog B, Huber K, Rennie AR. J Colloid Interface Sci 1994;164:370–81.

[280] Bergström M, Pedersen JS. J Phys Chem B 2000;104:4155–63.

[281] Beck R, Gradzielski M, Horbaschek K, Shah SS, Hoffmann H, Strunz P. J Colloid Interface Sci 2000;221:200–9.

[282] Oberdisse J, Couve C, Appell J, Berret JF, Ligoure C, Porte G. Langmuir 1996; 12:1212–8.

[283] Hao J, Yuan Z, Liu W, Hoffmann H. J Phys Chem B 2004;108:5105–12.

[284] Jonströmer M, Strey R. J Phys Chem 1992;96:5993–6000.

[285] Olsson U, Nakamura K, Kunieda H, Strey R. Langmuir 1996;12:3045–4.

[286] Hofland HEJ, Bouwstra JA, Gooris GS, Spies F, Talsma H, Junginger HE. J Colloid Interface Sci 1993;161:366–76.

[287] Montalvo G, Rodenas E, Valiente M. J Colloid Interface Sci 2000;227:171–5.

[288] Montalvo G, Rodenas E, Valiente M. J Colloid Interface Sci 1998;202:232–7.

[289] Würtz J, Hoffmann H. J Colloid Interface Sci 1995;175:304–17.

[290] Schomächer R, Strey R. J Phys Chem 1994;98:3908–12.

[291] Bergenholtz J, Wagner N. Langmuir 1996;12:3122–6.

[292] Khan A, Regev O. J Colloid Interface Sci 1996;182:95–109.

[293] Auguste F, Douliez JP, Belocq AM, Gulik-Krzywicki T. Langmuir 1996;13:666–72.

[294] Gomati R, Appell J, Bassereau P, Marignan J, Porte G. J Phys Chem 1987;91:6203–10.

[295] Strey R, Schomaecker R, Roux D, Nallet F, Olsson U. J Chem Soc Faraday Trans 1990;86:2253.

[296] Faucompre B, Lindman B. J Phys Chem 1987;91:383–9.

[297] Munkert U, Hoffmann H, Thunig C, Meyer HW, Richter W. Langmuir 1992;8:2629–38.

[298] Thunig C, Platz G, Hoffmann H. Ber Bunsenges Phys Chem 1992;96:667–77.

[299] Schepers FJ, Toet WK, Van de Pas JC. Langmuir 1993;9:956–61.

[300] Ristori S, Appell J, Porte G. Langmuir 1996;12:686–90.

[301] Okamura H, Imae T, Takagi K, Sawaki Y, Furusaka M. J Colloid Interface Sci 1996;180:98–105.

[302] Hoffmann H, Munkert U, Thunig C, Valiente M. J Colloid Interface Sci 1994;163:217–28.

[303] Wärnheim T, Bergenstahl B, Henriksson U, Malmvik AC, Nilsson P. J Colloid Interface Sci 1987;118:233.

[304] Regev O, Khan A. Prog Colloid Polym Sci 1994;97:298–301.

[305] Platz G, Thunig C, Pölike J, Kirchhoff W, Nickel D. Colloids Surf A 1994;88:113–22.

[306] Takeoka S, Mori K, Okhawa H, Sou K, Tsuchida E. J Am Chem Soc 2000;122:7927–35.

[307] Hao J, Liu W, Xu G, Zheng L. Langmuir 2003;19:10635–40.

[308] Wang X, Shen Y, Liang Y. Langmuir 2000;16:7538–40.

[309] Paleos CM, Tsiourvas D. Top Curr Chem 2003;227:1–29.

[310] Regev O, Kang C, Khan A. J Phys Chem 1994;98:6619–25.

[311] Hiemenz PC, Rajagopalan R. Principles of colloid and surfaces chemistry. New York: Marcel Dekker, Inc.; 1997. p. 39–57.

[312] Almgreen M. Austral J Chem 2003;56:959–70.

[313] Jung HT, Lee SY, Kaler EW, Coldren B, Zasadzinski JA. Proc Natl Acad Sci 2002;99:15318–22.

[314] Jung HT, Coldren B, Zasadzinski JA, Iampietro DJ, Kaler EW. Proc Natl Acad Sci 2001;98:1353–7.

[315] Pevzner S, Regev O, Lind A, Linden M. J Am Chem Soc 2003;125:652–3.

[316] Horbaschek K, Hoffmann H, Thunig C. J Colloid Interface Sci 1998;206:439–56.

[317] Glatter O, Hofer M. J Colloid Interface Sci 1988;122:496–506.

[318] Glatter O. Prog Colloid Polym Sci 1991;84:46–54.

[319] Bohren CF, Fuffman DR. Absorption and scattering of light by small particles. New York: John Wiley & Sons; 1983. p. 227–44.

[320] Radlinska EZ, Zemb TN, Dalbiez JP, Ninham BW. Langmuir 1993;9:2844–50.

[321] Kerker M. The scattering of light and other electromagnetic radiation. New York: Academic Press; 1969. p. 414–32.

[322] Schätzel K. Single-photon correlation techniques. In: Brown W, editor. Dynamic light scattering. the method and some applications. Oxford: Clarendon Press; 1993. p. 76–149.

[323] Brumberger H. Modern aspects of small angle scattering. London: Kluwer Academic Publishers; 1995. p. 107–80.

[324] Hess W. Diffusion coeficients in colloidal and polymeric solutions. In: Degiorgio V, Corti M, Giglio M, editors. Light scattering in liquids and macromolecular solutions. New York: Plenum Press; 1980. p. 31–50.

[325] Brown W, Nicolai T. Dynamic properties of polymer solutions. In: Brown W, editor. Dynamic light scattering. The method and some applications. Oxford: Clarendon Press; 1993. p. 272–318.

[326] Ford Jr NC. Light scattering apparatus. In: Pecora R, editor. Dynamic light scattering. Application of photon correlation spectroscopy. New York: Plenum Press; 1985. p. 7–58.

[327] Glatter O. Small angle scattering and light scattering. In: Linder P, Zemb T, editors. Neutron, X-ray and light scattering. Amsterdam: North Holland; 1991. p. 33–83.

[328] Chu B. Laser light scattering. London: Academic Press; 1974. p. 91.

[329] Pecora R. Dynamic light scattering. Application of photon correlation spectroscopy. New York: Plenum Press; 1985.

[330] Brown W. Dynamic light scattering. The method and some applications. Oxford: Clarendon Press; 1993.

[331] Dahneke BE. Measurements of suspended particles by quasi-elastic light scattering. New York: Wiley; 1983.

[332] Jones AR. Progr Energy Combust Sci 1999;25:1–53.

[333] Schnablegger H, Glatter O. Appl Opt 1991;30:4889–96.

[334] Koppel DE. J Chem Phys 1972;57:4814–20.

[335] Mao M, Huang J, Zhu B, Ye J. J Phys Chem B 2002;106:219–25.

[336] Shioi A, Hatton TA. Langmuir 2002;18:7341–8.

[337] Taneva SG, Patty PJ, Frisken BJ, Cornell RB. Biochemistry 2005; 44:9382–93.

[338] Glatter O. J Appl Chryst 1981;14:101–8.

[339] Bracewell R. Fourier transform and its applications. New York: McGraw-Hill; 1986.

[340] Debye P. Ann Phys 1915;46:809.

[341] Glatter O. J Appl Crystallogr 1979;12:166–75.

[342] Debye P, Büche AMJ. Appl Phys 1949;20:518.

[343] Porod G. Acta Phys Austriaca 1948;2:255–92.

[344] Glatter O, Kratky O. Data treatment. In: Glatter O, editor. Small-angle X-ray scattering. London: Academic Press; 1982.

[345] Kratky O, Porod G. Acta Phys Austriaca 1948;2:133–47.

[346] Glatter O, Kratky O. Interpretation. In: Glatter O, editor. Small-angle X-ray scattering. London: Academic Press; 1982.

[347] Glatter O. J Appl Crystallogr 1980;13:7–11.

[348] Šegota S, Horbaschek K, Težak Đ. Colloids Surf A 2001;193:109–16.

[349] Ne F, Testard F, Zemb Th, Grillo I. Langmuir 2003;19:8503–10.

[350] Glatter O. J Appl Chryst 1977;10:415–21.

[351] Glatter O, Strey R, Schubert K-V, Kaler EW. Ber Bunsenges Phys Chem 1996;100:323–35.

[352] Glatter O, Strey R, Schubert K-V, Kaler EW. J Chem Phys 1996;105:1175–88.

[353] Bergstrom M, Pedersen JS, Egelhaaf SU. J Phys Chem B 1999;103:9888–97.

[354] Kang SY, Seong BS, Han YS, Jung HT. Biomacromolecules 2003;4:360–5.

[355] Safran SA, Pincus PA, Andelman D, MacKintosh FC. Phys Rev A 1991;43:1071–8.

[356] Lin Z, Fu YC. J Colloid Interface Sci 1996;184:325–7.

[357] Luk AS, Kaler EW, Lee SP. Biochemistry 1997;36:5633–44.